

Joint Angle Estimation Error Analysis and 3D Positioning Algorithm Design for mmWave Positioning System

Tuo Wu, Cunhua Pan, Yijin Pan, Sheng Hong, Hong Ren, Maged ElKashlan,
Feng Shu and Jiangzhou Wang, *Fellow, IEEE*

Abstract

In this paper, we propose a comprehensive framework to jointly analyze the angle estimation error and design the three-dimensional (3D) positioning algorithm for a millimeter wave (mmWave) positioning system. First, we estimate the angles of arrival (AoAs) at the anchors by applying the two-dimensional discrete Fourier transform (2D-DFT) algorithm. Based on the property of the 2D-DFT algorithm, the angle estimation error is analyzed in terms of probability density functions (PDF). The analysis shows that the derived angle estimation error is non-Gaussian, which is different from the existing work. Second, the intricate expression of the PDF of the AoA estimation error is simplified by employing the first-order linear approximation of triangle functions. Then, we derive a complex expression for the variance based on the derived PDF. Specifically, for the azimuth estimation error, the variance is separately integrated according to the different non-zero intervals of the PDF. Finally, we apply the weighted least square (WLS) algorithm to estimate the 3D position of the MU by using the estimated AoAs and the obtained non-Gaussian variance. Extensive simulation results confirm that the derived angle estimation error is non-Gaussian, and also demonstrate the superiority of the proposed framework.

Index Terms

(Corresponding author: Cunhua Pan).

T. Wu and M. ElKashlan are with the School of Electronic Engineering and Computer Science at Queen Mary University of London, London E1 4NS, U.K. (Email: {tuo.wu, maged.elkashlan}@qmul.ac.uk). C. Pan, Y. Pan and H. Ren are with the National Mobile Communications Research Laboratory, Southeast University, Nanjing 210096, China. (Email: {cpan,panyj,hren}@seu.edu.cn). S. Hong is with Information Engineering School of Nanchang University, Nanchang 330031, China. (Email: shenghong@ncu.edu.cn). F. Shu is with the School of Electronic and Optical Engineering, Nanjing University of Science and Technology, Nanjing 210094, China, and also with the School of Information and Communication Engineering, Hainan University, Haikou 570228, China.(E-mail: shufeng0101@163.com). J. Wang is with the School of Engineering, University of Kent, UK. (e-mail: J.Z.Wang@kent.ac.uk).

Millimeter wave (mmWave), angles of arrival (AoAs), non-Gaussian, positioning.

I. INTRODUCTION

As an important requirement for the sixth generation (6G) wireless networks, high-accuracy positioning service is of great importance in a wide range of applications [1], such as automated driving vehicles [2], smart factory [3] and virtual reality [4]. For example, it is predicted that the 2020s will be the first decade for automated driving vehicles with the positioning accuracy at decimeter level [5]. However, the positioning accuracy of the prevalent global positioning system (GPS) is about 5 meters even in ideal conditions [6], which cannot meet the stringent requirement on positioning accuracy for these thriving applications [7]. Therefore, network-based positioning systems are emerging as a promising alternative to GPS in 6G networks [8].

In current wireless positioning networks, the millimeter wave (mmWave) technique [9] can provide an extremely highly-accurate estimation of channel parameters, such as the channel gain, time delays, and angle of arrival (AoA). These parameters can be used to estimate the position of the mobile user (MU). Therefore, it is of much interest to explore positioning algorithms for the mmWave positioning systems. Typically, positioning algorithms work through the following two steps. First, channel parameters can be acquired through some estimation methods [10]–[12]. Second, positioning algorithms can be designed accordingly. Specifically, expressions of the complex non-linear geometric relationships between the channel parameters and the position coordinates are first derived [13]. Then, the estimation error of the channel parameters and the non-linear geometric relationships are jointly utilized to derive the non-linear equations [14]. Finally, the position of the MU is determined by solving the equations using iterative or non-iterative algorithms. From the above-mentioned positioning steps, the estimation error of the channel parameters can directly determine the positioning accuracy. In general, different methods for estimating different channel parameters lead to different types of parameter estimation errors [15].

To date, mmWave positioning systems have attracted extensive research attention [16]–[21]. To reduce the high computational complexity due to a large number of antennas, [16] proposed a novel channel compression method for the mmWave positioning systems. In [17], the successive localization and beamforming scheme was proposed to estimate the long-term MU location and the instantaneous channel state for the mmWave multiple-input multiple-output (MIMO) communications. To provide an analytical performance validation, [18] studied the theoretical

performance bounds (i.e., Cramér-Rao lower bounds (CRLB)) for positioning, and evaluated the impact of the number of reflecting elements and the phase shifts of reconfigurable intelligent surface (RIS) on the positioning estimation accuracy. Alouini *et al.* derived the CRLB for assessing the performance of synchronous and asynchronous signaling schemes and proposed an optimal closed-form expression of the reflecting phase shifts of the RIS for joint communication and localization [19]. The authors of [20] demonstrated that accurate estimates of the position of an unknown node can be determined using estimates of time of arrival (ToA), and AoA, as well as data fusion or machine learning. [21] considered the channel estimation problem and the channel-based wireless applications in MIMO orthogonal frequency division multiplexing (OFDM) systems assisted by RISs.

However, the above contributions assumed that the estimation error of the channel parameters follows the Gaussian distribution, which is inconsistent with practical scenarios. In practice, the distribution of these parameters depends on the practical estimation methods (e.g., 2D-DFT algorithm [22]), which may not follow the Gaussian distribution. Therefore, existing positioning algorithms and performance analysis may not be applicable when considering practical channel parameter estimation methods. Hence, it is necessary to model the estimation error of the estimated channel parameters, so that the position of the MU can be estimated based on the estimation error.

In this paper, we aim to propose a complete framework to jointly analyze the angle estimation and design the three-dimensional (3D) positioning algorithm for the mmWave positioning system. Our main contributions are summarized as follows:

- 1) We propose a comprehensive framework to jointly analyze the angle estimation and design the 3D positioning algorithm for the mmWave positioning system. Specifically, we first estimate the AoAs at the anchors by applying the 2D-DFT algorithm. Then, we derive the closed-form expression of the PDF of the estimation error. We further derive the variance of the estimation error based the PDF. Finally, by using the estimated AoAs and the derived variance, we apply the weighted least square (WLS) algorithm to estimate the 3D position of the MU.
- 2) The estimated AoAs are first derived in closed-form based on the 2D-DFT method. Based on the expression of estimation, we find that the angle estimation error at the anchors depends on the search grid, the panel size of the anchors, and the number of antennas of the anchors. Moreover, due to the property of 2D-DFT, the angle estimation error follows

the uniform distribution.

- 3) According to the uniform distribution of the estimation error of azimuth and elevation, the angle estimation error is characterized in terms of the PDF, which is non-Gaussian. To be specific, we first derive the PDF by using the geometric relationship between the AoAs and their triangle functions. Then, we simplify the complex geometric expression of the PDF by employing the first-order linear approximation of the triangle function. For the azimuth angle estimation, we provide an algorithm to derive and approximate the PDF expression of its estimation error.
- 4) Based on the PDF of estimation error, we theoretically derive the variance of the angle estimation error. Since the PDF of the azimuth estimation error has three different non-zero intervals, we separately calculate the integral in the different intervals according to the variance calculation formula.
- 5) Simulation results verify the accuracy of the derived results and demonstrate the superiority of the proposed framework. We observe that the variance decreases with the number of elements, which means that increasing the number of anchor antennas improves the estimation accuracy.

The remainder of the paper is organized as follows. The system model for the mmWave positioning system is described in Section II. The details of the whole framework are given in Section III. The procedures of estimating angles are given in Section IV. Section V derives the PDF in more details. Section VI calculates the variance. The positioning algorithm is given in Section VII. Simulation results are given in Section VIII. Section IX concludes the work of this paper.

II. SYSTEM MODEL

Consider a mmWave time division duplex (TDD) 3D positioning system, where an MU sends pilot signals to the anchors to locate the MU. We assume that there are I anchors, each of which is equipped with a uniform planar array (UPA) with $N_{y,z} = N_y \times N_z$ antennas, where N_y and N_z denote the numbers of antennas along the y-axis and z-axis, respectively. The MU is equipped with a single antenna.

As shown in Fig. 1, the anchors are placed parallel to the y-o-z plane with the center located at $\mathbf{s}_i = [x_i, y_i, z_i]^T$, $i \in [1, \dots, I]$. The true location of the MU is $\mathbf{q} = [x_q, y_q, z_q]^T$. The estimated location of the MU is denoted as $\hat{\mathbf{q}} = [\hat{x}_q, \hat{y}_q, \hat{z}_q]^T$. Generally, once the anchors are deployed,

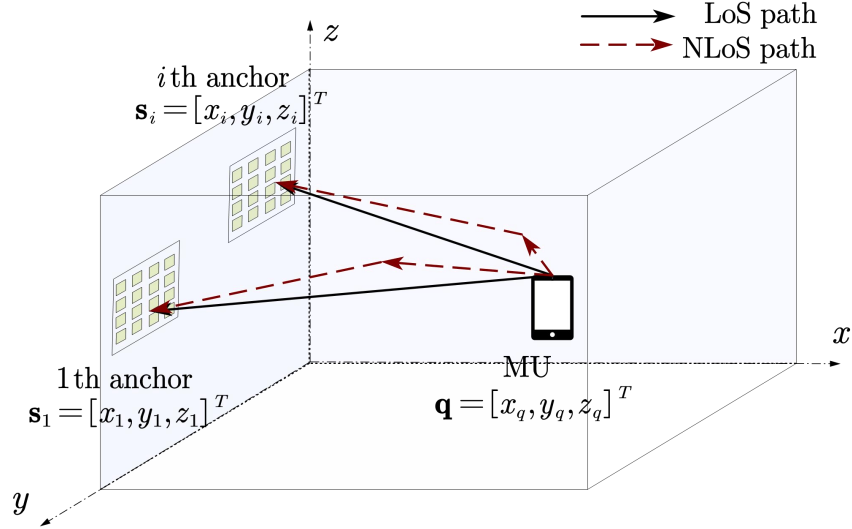


Fig. 1: System model of considered mmWave positioning system.

the coordinate \mathbf{s}_i are known and invariant. In order to locate the MU, we need to obtain the estimated $\hat{\mathbf{q}}$.

Assuming that the number of propagation paths between the MU and the i th anchor is N_i , the AoA of the n_i th path from the MU to the i th anchor can be decomposed into the elevation angle $0 \leq \Theta_{n_i} \leq \pi$ in the vertical direction, and the azimuth angle $0 \leq \Phi_{n_i} \leq \pi$ in the horizontal direction, respectively. As a result, the array response vector at the i th anchor of the n_i th path can be expressed as

$$\mathbf{a}(\Theta_{n_i}, \Phi_{n_i}) = \mathbf{a}_e(\Phi_{n_i}) \otimes \mathbf{a}_a(\Theta_{n_i}, \Phi_{n_i}), \quad (1)$$

where \otimes denotes the Kronecker product. Moreover, we have

$$\mathbf{a}_e(\Phi_{n_i}) = [1, e^{\frac{-j2\pi d_r \sin \Phi_{n_i}}{\lambda_c}}, \dots, e^{\frac{-j2\pi(M_x-1)d_r \sin \Phi_{n_i}}{\lambda_c}}]^T, \quad (2)$$

and

$$\mathbf{a}_a(\Theta_{n_i}, \Phi_{n_i}) = [1, e^{\frac{-j2\pi d_r \cos \Theta_{n_i} \cos \Phi_{n_i}}{\lambda_c}}, \dots, e^{\frac{-j2\pi(M_z-1)d_r \cos \Theta_{n_i} \cos \Phi_{n_i}}{\lambda_c}}]^T, \quad (3)$$

where d_r and λ_c denote the distance between the antennas of the anchors and the carrier wavelength, respectively. Then, the channel between the MU and the i th anchor, denoted as

\mathbf{h}_i , can be modeled as

$$\mathbf{h}_i = \sum_{n_i=1}^{N_i} \alpha_{n_i} \mathbf{a}(\Theta_{n_i}, \Phi_{n_i}) = \underbrace{\alpha_{L,i} \mathbf{a}(\Theta_{L,i}, \Phi_{L,i})}_{LoS} + \underbrace{\sum_{n_i=2}^{N_i} \alpha_{n_i} \mathbf{a}(\Theta_{n_i}, \Phi_{n_i})}_{NLoS}, \quad (4)$$

where α_{n_i} denotes the complex channel gain of n_i th path. Moreover, $\alpha_{L,i}$, $\Theta_{L,i}$, and $\Phi_{L,i}$ denote the complex channel gain, the elevation AoA, and the azimuth AoA of the line-of-sight (LoS) path, respectively. As we can see from (4), channel components of \mathbf{h}_i can be categorized into two types, namely *LoS* and *NLoS*. LoS path component is the direct path between the anchors and the MU, non-line-of-sight (NLoS) path component consists of the paths between the anchors and the MU reflected by scatters, e.g., walls, human bodies, and etc. Moreover, according to [23], the complex channel gain of LoS is given by

$$\alpha_{L,i} = \frac{\lambda_c e^{-j2\pi d_{L,i}}}{4\pi d_{L,i}}, \quad (5)$$

where $d_{L,i}$ is the distance between the i th anchor and the MU.

III. JOINT ANGLE ESTIMATION ANALYSIS AND 3D POSITIONING ALGORITHM DESIGN

In the existing works concerning the positioning algorithm design, for tractability, the estimation error of channel parameters is assumed to be additive zero-mean complex Gaussian noise. However, in practice, the distribution of these channel parameters depends on the practical estimation methods, which may not follow the Gaussian distribution. To investigate the impact of the practical estimation error of the channel parameters, we propose to design a comprehensive framework to jointly analyze the angle estimation error and estimate the 3D position of the MU.

Based on the 2D-DFT angle estimation technique, the angle estimation error analysis and 3D positioning algorithm design is investigated in this paper. First, we apply the 2D-DFT algorithm to estimate $(\Theta_{L,i}, \Phi_{L,i})$ ¹. Then, based on the estimation of the AoAs, we first derive the PDF of the angle estimation error, based on which the closed-form expression of the variance of the angle estimation error is derived. Finally, we apply the WLS algorithm to estimate the 3D position of the MU by using the estimated AoAs and the derived variance.

¹As NLoS path component usually varies fast and its weight to the channel is marginal, especially in the mmWave band, we are more interested in LoS path. Hence, we intend to estimate the path parameter $(\Theta_{L,i}, \Phi_{L,i})$ of the LoS component from the MU to the anchors, which can be used to derive the position of the MU.

The details of the proposed framework are summarized in Algorithm 1. The descriptions of each step of the proposed framework will be introduced in the following sections.

Algorithm 1 Joint Angle Estimation Error Analysis and 3D Positioning Framework

- 1: Estimate $(\Theta_{L,i}, \Phi_{L,i})$ by using the 2D-DFT estimation algorithm;
 - 2: Derive the PDF of the angle estimation error;
 - 3: Derive the closed-form expression of the variance of the angle estimation error;
 - 4: Estimate the 3D position of the MU by using the variance of the angle estimation error.
-

IV. ANGLE ESTIMATION

The first step of the proposed framework is to estimate $(\Theta_{L,i}, \Phi_{L,i})$. Hence, in this section, we apply the 2D-DFT algorithm [12] to estimate the AoA at the anchors. For the sake of illustration, we consider the estimation errors only for the noise-free scenario similar to [12] and [24], the performance of which is roughly the same as the general scenarios with sufficiently high received signal to noise ratio (SNR).

A. Initial Angle Estimation

According to the expression of $\mathbf{a}(\Theta_{L,i}, \Phi_{L,i})$ in (1), $\mathbf{a}(\Theta_{L,i}, \Phi_{L,i})$ can be further derived as

$$\mathbf{a}(\Theta_{L,i}, \Phi_{L,i}) = \text{vec}\{\mathbf{A}(\Theta_{L,i}, \Phi_{L,i})\} = \text{vec}\{\mathbf{a}_e(\Phi_{L,i})\mathbf{a}_a(\Theta_{L,i}, \Phi_{L,i})\}. \quad (6)$$

To estimate the AoA at the i th anchor, we define two normalized DFT matrices \mathbf{F}_{N_y} and \mathbf{F}_{N_z} , elements of which are written as $[\mathbf{F}_{N_y}]_{b_i b'_i} = e^{-j\frac{2\pi}{N_y} b_i b'_i}$ ($b_i, b'_i = 0, 1, \dots, N_y - 1$) and $[\mathbf{F}_{N_z}]_{q_i q'_i} = e^{-j\frac{2\pi}{N_z} q_i q'_i}$ ($q_i, q'_i = 0, 1, \dots, N_z - 1$), respectively. Meanwhile, let us define $u_{L,i} = \frac{2\pi d_r \cos \Theta_{L,i} \cos \Phi_{L,i}}{\lambda_c}$ and $v_{L,i} = \frac{2\pi d_r \sin \Phi_{L,i}}{\lambda_c}$. Then, we define the normalized 2D-DFT of the matrix $\mathbf{A}(\Theta_{L,i}, \Phi_{L,i})$ in (6) as $\mathbf{A}_{DFT}(\Theta_{L,i}, \Phi_{L,i}) = \mathbf{F}_{N_y} \mathbf{A}(\Theta_{L,i}, \Phi_{L,i}) \mathbf{F}_{N_z}$, whose (b_i, q_i) th element is calculated as

$$\begin{aligned} [\mathbf{A}_{DFT}(\Theta_{L,i}, \Phi_{L,i})]_{b_i q_i} &= \sum_{n_y=0}^{N_y-1} \sum_{n_z=0}^{N_z-1} [\mathbf{A}(\Theta_{L,i}, \Phi_{L,i})]_{b_i q_i} e^{-j2\pi(\frac{b_i n_y}{N_y} + \frac{q_i n_z}{N_z})} \\ &= e^{j\frac{N_y-1}{2}(u_{L,i} - \frac{2\pi b_i}{N_y})} e^{j\frac{N_z-1}{2}(v_{L,i} - \frac{2\pi q_i}{N_z})} \\ &\quad \times \frac{\sin(\pi b_i - \frac{N_y u_{L,i}}{2})}{\sin((\pi b_i - \frac{N_y u_{L,i}}{2})/N_y)} \cdot \frac{\sin(\pi q_i - \frac{N_z v_{L,i}}{2})}{\sin((\pi q_i - \frac{N_z v_{L,i}}{2})/N_z)}. \end{aligned} \quad (7)$$

When the number of reflecting elements becomes infinite, i.e., $N_y \rightarrow \infty$, $N_z \rightarrow \infty$, there always exist some integers $b_{n_i} = \frac{N_y u_{L,i}}{2\pi}$, $q_{n_i} = \frac{N_z v_{L,i}}{2\pi}$ such that $[\mathbf{A}_{DFT}(\Theta_{L,i}, \Phi_{L,i})]_{b_{n_i} q_{n_i}} = 1$, while the other elements are all zero. Therefore, all power is concentrated on the (b_{n_i}, q_{n_i}) th element and $\mathbf{A}_{DFT}(\Theta_{L,i}, \Phi_{L,i})$ is a sparse matrix. However, the anchor size could not be infinitely large, thus $\frac{N_y u_{L,i}}{2\pi}$ and $\frac{N_z v_{L,i}}{2\pi}$ may not be integers in general, which leads to the channel power leakage from the (b_{n_i}, q_{n_i}) th element to its adjacent element. However, $\mathbf{A}_{DFT}(\Theta_{L,i}, \Phi_{L,i})$ can still be approximated as a sparse matrix with the most power concentrated around the (b_{n_i}, q_{n_i}) th element. Therefore, the peak power position of $\mathbf{A}_{DFT}(\Theta_{L,i}, \Phi_{L,i})$ is still useful for estimating the AoAs at the anchor. Then, the initial estimation is derived as follows:

$$\begin{aligned} \cos \hat{\Theta}_{L,i}^{ini} \cos \hat{\Phi}_{L,i}^{ini} &= \frac{\lambda_c b_{n_i}}{N_y d_r}, \\ \sin \hat{\Phi}_{L,i}^{ini} &= \frac{\lambda_c q_{n_i}}{N_z d_r}, \end{aligned} \quad (8)$$

where $\hat{\Theta}_{L,i}^{ini}$ and $\hat{\Phi}_{L,i}^{ini}$ denote the initial estimated angles at the anchor.

B. Fine Angle Estimation

The resolution of the estimated $\sin \hat{\Phi}_{L,i}^{ini}$ and $\cos \hat{\Theta}_{L,i}^{ini} \cos \hat{\Phi}_{L,i}^{ini}$ is limited by the half of the DFT interval. In order to improve the estimation accuracy, angle rotation is provided to solve the mismatch issue in this subsection [22].

Let us define the angle rotation matrix of $\mathbf{A}(\Theta_{L,i}, \Phi_{L,i})$ as $\mathbf{A}^{ro}(\Theta_{L,i}, \Phi_{L,i})$, expressed as

$$\mathbf{A}^{ro}(\Theta_{L,i}, \Phi_{L,i}) = \mathbf{U}_{N_y}(\tilde{\omega}_{1,i}) \mathbf{A}(\Theta_{L,i}, \Phi_{L,i}) \mathbf{U}_{N_z}(\tilde{\omega}_{2,i}), \quad (9)$$

where the diagonal matrices $\mathbf{U}_{N_y}(\tilde{\omega}_{1,i})$ and $\mathbf{U}_{N_z}(\tilde{\omega}_{2,i})$ are given by

$$\begin{aligned} \mathbf{U}_{N_y}(\tilde{\omega}_{1,i}) &= \text{Diag}\{1, e^{j\tilde{\omega}_{1,i}}, \dots, e^{j(N_y-1)\tilde{\omega}_{1,i}}\}, \\ \mathbf{U}_{N_z}(\tilde{\omega}_{2,i}) &= \text{Diag}\{1, e^{j\tilde{\omega}_{2,i}}, \dots, e^{j(N_z-1)\tilde{\omega}_{2,i}}\}, \end{aligned} \quad (10)$$

with $\tilde{\omega}_{1,i} \in [-\pi/N_y, \pi/N_y]$ and $\tilde{\omega}_{2,i} \in [-\pi/N_z, \pi/N_z]$ being the angle rotation parameters. By using the angle rotation operation, the (b_i, q_i) th element of the 2D-DFT of the rotated matrix

$\mathbf{A}_{DFT}^{ro}(\Theta_{L,i}, \Phi_{L,i})$ is calculated as

$$\begin{aligned}
[\mathbf{A}_{DFT}^{ro}(\Theta_{L,i}, \Phi_{L,i})]_{b_i q_i} &= \sum_{n_y=0}^{N_y-1} \sum_{n_z=0}^{N_z-1} [\mathbf{A}(\Theta_{L,i}, \Phi_{L,i})]_{b_i q_i} e^{-j2\pi(\frac{b_i n_y}{N_y} + \frac{q_i n_z}{N_z})} e^{j2\pi(\frac{\tilde{\omega}_{1,i} n_y}{2\pi} + \frac{\tilde{\omega}_{2,i} n_z}{2\pi})} \\
&= e^{j\frac{N_y-1}{2}(u_{L,i} + \tilde{\omega}_{1,i} - \frac{2\pi b_i}{N_y})} e^{j\frac{N_z-1}{2}(v_{L,i} + \tilde{\omega}_{2,i} - \frac{2\pi q_i}{N_z})} \\
&\quad \times \frac{\sin(\pi b_i - \frac{N_y u_{L,i}}{2} - \frac{N_y \tilde{\omega}_{1,i}}{2})}{\sin((\pi b_i - \frac{N_y u_{L,i}}{2} - \frac{N_y \tilde{\omega}_{1,i}}{2})/N_y)} \cdot \frac{\sin(\pi q_i - \frac{N_z v_{L,i}}{2} - \frac{N_z \tilde{\omega}_{2,i}}{2})}{\sin((\pi q_i - \frac{N_z v_{L,i}}{2} - \frac{N_z \tilde{\omega}_{2,i}}{2})/N_z)},
\end{aligned} \tag{11}$$

where $\tilde{\omega}_{1,i}$ and $\tilde{\omega}_{2,i}$ could be optimized with the one-dimensional search. Then, we could obtain the estimated results as

$$\begin{aligned}
\cos \hat{\Theta}_{L,i} \cos \hat{\Phi}_{L,i} &= \frac{\lambda_c b_{n_i}}{N_y d_r} - \frac{\lambda_c \tilde{\omega}_{1,i}}{2\pi d_r}, \\
\sin \hat{\Phi}_{L,i} &= \frac{\lambda_c q_{n_i}}{N_z d_r} - \frac{\lambda_c \tilde{\omega}_{2,i}}{2\pi d_r},
\end{aligned} \tag{12}$$

where $\hat{\Theta}_{L,i}$ and $\hat{\Phi}_{L,i}$ denote the final estimated azimuth and elevation AoAs after angle rotation, respectively. Furthermore, $\hat{\Theta}_{L,i}$ and $\hat{\Phi}_{L,i}$ could be expressed as

$$\begin{aligned}
\hat{\Phi}_{L,i} &= \arcsin\left(\frac{\lambda_c b_{n_i}}{N_y d_r} - \frac{\lambda_c \tilde{\omega}_{1,i}}{2\pi d_r}\right), \\
\hat{\Theta}_{L,i} &= \arccos\left(\left(\frac{\lambda_c b_{n_i}}{N_y d_r} - \frac{\lambda_c \tilde{\omega}_{1,i}}{2\pi d_r}\right) / \sqrt{\left(1 - \left(\frac{\lambda_c q_{n_i}}{N_z d_r} - \frac{\lambda_c \tilde{\omega}_{2,i}}{2\pi d_r}\right)^2\right)}\right).
\end{aligned} \tag{13}$$

V. DERIVATION OF THE PDF OF ANGLE ESTIMATION ERROR

In this section, as the second step of the proposed framework, we derive the PDF of the angle estimation error, which will be used for deriving the variance of the angle estimation error. To obtain the PDF of the angle estimation error, the first step is to derive the PDF of $\tilde{\Phi}_{L,i}$ based on the estimated angle $\hat{\Phi}_{L,i}$ and the property of the 2D-DFT. Then, the second step is to design an algorithm by deriving the PDF of $\tilde{\Theta}_{L,i}$ based on the estimated angle $\hat{\Theta}_{L,i}$ and the property of the 2D-DFT. The details are given as follows:

A. PDF of $\tilde{\Phi}_{L,i}$

Based on the above section, we can find that $\tilde{\omega}_{2,i}$ could be obtained by the one-dimensional search in the interval of $[-\frac{\pi}{N_z}, \frac{\pi}{N_z}]$. We assume that there are $S_{2,i}$ grids points in the interval

$[-\frac{\pi}{N_z}, \frac{\pi}{N_z}]$ and $s_{2,i} \in \{1, \dots, S_{2,i}\}$ is the optimal point. Therefore, the optimal solution for the one-dimensional search is $\tilde{\omega}_{2,i} = \frac{2\pi s_{2,i}}{N_z S_{2,i}}$, and the estimation of $\sin \Phi_{L,i}$ is thus written as

$$\sin \hat{\Phi}_{L,i} = \frac{\lambda_c q_{n_i}}{N_z d_r} - \frac{\lambda_c \tilde{\omega}_{2,i}}{2\pi d_r} = \frac{\lambda_c q_{n_i}}{N_z d_r} - \frac{\lambda_c s_{2,i}}{N_z d_r S_{2,i}}. \quad (14)$$

For notation simplicity, let us define $\hat{Y}_i = \sin \hat{\Phi}_{L,i}$ and $Y_i = \sin \Phi_{L,i}$. Then, the estimation of $\Phi_{L,i}$ could be expressed as

$$\hat{\Phi}_{L,i} = \arcsin \hat{Y}_i = \arcsin \left(\frac{\lambda_c q_{n_i}}{N_z d_r} - \frac{\lambda_c s_{2,i}}{N_z d_r S_{2,i}} \right). \quad (15)$$

According to (14) and the property of the one-dimensional search method, the value of Y_i follows the uniform distribution within the region of $[\hat{Y}_i - a_i, \hat{Y}_i + a_i]$, where $a_i = \frac{\lambda_c}{2N_z d_r S_{2,i}}$, which is given by

$$f_{Y_i}(y) = \begin{cases} \frac{1}{2a_i}, & \hat{Y}_i - a_i \leq y \leq \hat{Y}_i + a_i \\ 0, & \text{others.} \end{cases} \quad (16)$$

By denoting the estimation error of Y_i as \tilde{Y}_i , we have $\hat{Y}_i = Y_i + \tilde{Y}_i$. Then, the distribution of \tilde{Y}_i is given by

$$f_{\tilde{Y}_i}(\tilde{y}) = \begin{cases} \frac{1}{2a_i}, & -a_i \leq \tilde{y} \leq a_i \\ 0, & \text{others.} \end{cases} \quad (17)$$

Since $\Phi_{L,i} = \arcsin Y_i$, the cumulative density function (CDF) of $\Phi_{L,i}$ is derived as

$$F_{\Phi_{L,i}}(\phi_{L,i}) = \Pr(\Phi_{L,i} \leq \phi_{L,i}) = \Pr(\arcsin Y_i \leq \phi_{L,i}) = \Pr(Y_i \leq \sin \phi_{L,i}). \quad (18)$$

By assuming that $\Phi_{L,i} \in (-\frac{\pi}{2}, \frac{\pi}{2})$, the PDF of $\Phi_{L,i}$ could be derived as

$$\begin{aligned} f_{\Phi_{L,i}}(\phi_{L,i}) &= \frac{\partial F_{\Phi_{L,i}}(\phi_{L,i})}{\partial \phi_{L,i}} = \cos \phi_{L,i} f_{Y_i}(\sin \phi_{L,i}) \\ &= \begin{cases} \frac{\cos \phi_{L,i}}{2a_i}, & \arcsin(\hat{Y}_i - a_i) \leq \phi_{L,i} \leq \arcsin(\hat{Y}_i + a_i) \\ 0, & \text{others.} \end{cases} \end{aligned} \quad (19)$$

As we have $\hat{\Phi}_{L,i} = \Phi_{L,i} + \tilde{\Phi}_{L,i}$, the CDF of the estimation error $\tilde{\Phi}_{L,i}$ is calculated as

$$\begin{aligned} F_{\tilde{\Phi}_{L,i}}(\tilde{\phi}_{L,i}) &= \Pr(\tilde{\Phi}_{L,i} \leq \tilde{\phi}_{L,i}) = \Pr(\hat{\Phi}_{L,i} - \Phi_{L,i} \leq \tilde{\phi}_{L,i}) \\ &= \Pr(\Phi_{L,i} \geq \hat{\Phi}_{L,i} - \tilde{\phi}_{L,i}) = 1 - \Pr(\Phi_{L,i} \leq \hat{\Phi}_{L,i} - \tilde{\phi}_{L,i}). \end{aligned} \quad (20)$$

Define $a_{1,i} = \arcsin(\hat{Y}_i + a_i)$ and $a_{2,i} = \arcsin(\hat{Y}_i - a_i)$. Based on (20), the PDF of $\tilde{\Phi}_{L,i}$ is written as

$$\begin{aligned} f_{\tilde{\Phi}_{L,i}}(\tilde{\phi}_{L,i}) &= \frac{\partial F_{\tilde{\Phi}_{L,i}}(\tilde{\phi}_{L,i})}{\partial \tilde{\phi}_{L,i}} = f_{\Phi_{L,i}}(\hat{\Phi}_{L,i} - \tilde{\phi}_{L,i}) \\ &= \begin{cases} \frac{\cos(\hat{\Phi}_{L,i} - \tilde{\phi}_{L,i})}{2a_i}, & \hat{\Phi}_{L,i} - a_{1,i} \leq \tilde{\phi}_{L,i} \leq \hat{\Phi}_{L,i} - a_{2,i} \\ 0, & \text{others.} \end{cases} \end{aligned} \quad (21)$$

Moreover, as the estimation techniques are relatively mature, it is assumed that the estimation error is very small. Therefore, we have $\sin(\tilde{\phi}_{L,i}) \approx \tilde{\phi}_{L,i}$ and $\cos(\tilde{\phi}_{L,i}) \approx 1$. Consequently, we have the following approximation:

$$\cos(\hat{\Phi}_{L,i} - \tilde{\phi}_{L,i}) = \cos \hat{\Phi}_{L,i} \cos \tilde{\phi}_{L,i} + \sin \hat{\Phi}_{L,i} \sin \tilde{\phi}_{L,i} \approx \cos \hat{\Phi}_{L,i} + \tilde{\phi}_{L,i} \sin \hat{\Phi}_{L,i}. \quad (22)$$

Then, the PDF of $\tilde{\Phi}_{L,i}$ is approximated as

$$f_{\tilde{\Phi}_{L,i}}(\tilde{\phi}_{L,i}) \approx \begin{cases} \frac{\cos \hat{\Phi}_{L,i} + \tilde{\phi}_{L,i} \sin \hat{\Phi}_{L,i}}{2a_i}, & \hat{\Phi}_{L,i} - a_{1,i} \leq \tilde{\phi}_{L,i} \leq \hat{\Phi}_{L,i} - a_{2,i} \\ 0, & \text{others.} \end{cases} \quad (23)$$

B. PDF of $\tilde{\Theta}_{L,i}$

In this subsection, we derive the PDF of the estimation error $\tilde{\Theta}_{L,i}$. As the derivations are complicated, we summarize the main procedure in Algorithm 2.

Algorithm 2 Algorithm of deriving the PDF of $\tilde{\Phi}_{L,i}$

- 1: Derive the PDF of $\cos \Phi_{L,i}$ by using the PDF of \tilde{Y}_i in (17);
 - 2: Derive the PDF of $\cos \Theta_{L,i}$ for two cases by using the PDF of $\cos \Phi_{L,i}$ in (30) and the PDF of $\cos \Phi_{L,i} \cos \Theta_{L,i}$ in (32);
 - 3: Derive the PDF of $\tilde{\Theta}_{L,i}$ based on the two cases of the PDF of $\cos \Theta_{L,i}$ in (41) and (42).
-

1) *PDF of $\cos \Phi_{L,i}$* : First of all, we need to derive the PDF of $\cos \Phi_{L,i}$, so that the PDF of $\cos \Theta_{L,i}$ could be calculated.

Let $X_i = \cos \Phi_{L,i}$, which can be expressed as a function of \tilde{Y}_i as follows:

$$X_i = \cos \Phi_{L,i} = \sqrt{1 - \sin^2 \Phi_{L,i}} = \sqrt{1 - Y_i^2} = \sqrt{1 - (\hat{Y}_i - \tilde{Y}_i)^2}. \quad (24)$$

By defining the estimation of X_i as $\hat{X}_i = \cos \hat{\Phi}_{L,i} = X_i + \tilde{X}_i$, the estimation error \tilde{X}_i could be calculated as:

$$\tilde{X}_i = \hat{X}_i - \sqrt{1 - (\hat{Y}_i - \tilde{Y}_i)^2}. \quad (25)$$

However, the expression (25) is complicated and thus challenging to derive a compact form of the PDF of \tilde{X}_i . Fortunately, since the value of \tilde{Y}_i is relatively small, we can approximate \tilde{X}_i in (25) by using the Taylor expansion, which is given by

$$\tilde{X}_i = \sqrt{1 - \hat{Y}_i^2} - \sqrt{1 - (\hat{Y}_i - \tilde{Y}_i)^2} \approx \sqrt{1 - \hat{Y}_i^2} - \left((1 - \hat{Y}_i^2)^{\frac{1}{2}} + \frac{\tilde{Y}_i \cdot \hat{Y}_i}{(1 - \hat{Y}_i^2)^{\frac{1}{2}}} \right) = -\frac{\hat{Y}_i}{\hat{X}_i} \tilde{Y}_i. \quad (26)$$

Utilizing (26), the CDF of \tilde{X}_i could be calculated as

$$F_{\tilde{X}_i}(\tilde{x}_i) = \Pr(\tilde{X}_i \leq \tilde{x}_i) \approx \Pr\left(-\frac{\hat{Y}_i}{\hat{X}_i} \tilde{Y}_i \leq \tilde{x}_i\right) = \Pr\left(\tilde{Y}_i \geq -\frac{\hat{X}_i}{\hat{Y}_i} \tilde{x}_i\right) = 1 - \Pr\left(\tilde{Y}_i \leq -\frac{\hat{X}_i}{\hat{Y}_i} \tilde{x}_i\right). \quad (27)$$

Then, by using (27), the PDF of \tilde{X}_i could be calculated as

$$f_{\tilde{X}_i}(\tilde{x}_i) = -\left(-\frac{\hat{X}_i}{\hat{Y}_i}\right) f_{\tilde{Y}_i}\left(-\frac{\hat{X}_i}{\hat{Y}_i} \tilde{x}_i\right) = \begin{cases} \frac{\hat{X}_i}{2a_i \hat{Y}_i}, & -\frac{\hat{Y}_i}{\hat{X}_i} a_i \leq \tilde{x}_i \leq \frac{\hat{Y}_i}{\hat{X}_i} a_i \\ 0, & \text{others.} \end{cases} \quad (28)$$

Furthermore, by using $\hat{X}_i = X_i + \tilde{X}_i$, the CDF of X_i can be calculated as

$$F_{X_i}(x_i) = \Pr(X_i \leq x_i) = \Pr(\hat{X}_i - \tilde{X}_i \leq x_i) = \Pr(\tilde{X}_i \geq \hat{X}_i - x_i) = 1 - \Pr(\tilde{X}_i \leq \hat{X}_i - x_i). \quad (29)$$

By using (28) and (29), the PDF of X_i could be written as

$$f_{X_i}(x_i) = \frac{\partial F_{X_i}(x_i)}{\partial x_i} = f_{\tilde{X}_i}(\hat{X}_i - x_i) = \begin{cases} \frac{\hat{X}_i}{2a_i \hat{Y}_i}, & \hat{X}_i - \frac{\hat{Y}_i}{\hat{X}_i} a_i \leq x_i \leq \hat{X}_i - \frac{\hat{Y}_i}{\hat{X}_i} a_i \\ 0, & \text{others.} \end{cases} \quad (30)$$

2) *PDF of $\cos \Theta_{L,i}$* : By using the PDF of $\cos \Phi_{L,i}$ and $\cos \Phi_{L,i} \cos \Theta_{L,i}$, we can derive the PDF of $\cos \Theta_{L,i}$ as follows.

Firstly, from the above section, we know that $\tilde{\omega}_{1,i}$ could be obtained by using the one-dimensional search in the interval of $[-\frac{\pi}{N_y}, \frac{\pi}{N_y}]$. Similarly, we assume that there are S_1 grids points in the interval $[-\frac{\pi}{N_y}, \frac{\pi}{N_y}]$ and $s_{1,i} \in \{1, \dots, S_{1,i}\}$ is the optimal point. Therefore, the optimal solution for the one-dimensional search is $\tilde{\omega}_{1,i} = \frac{2\pi s_{1,i}}{N_y S_{1,i}}$, and the estimated $\cos \Phi_{L,i} \cos \Theta_{L,i}$ is given by

$$\hat{Z} = \cos \hat{\Theta}_{L,i} \cos \hat{\Phi}_{L,i} = \frac{\lambda_c b_{n_i}}{N_y d_1} - \frac{\lambda_c \tilde{\omega}_{1,i}}{2\pi d_r} = \frac{\lambda_c b_{n_i}}{N_y d_r} - \frac{\lambda_c s_{1,i}}{N_y d_r S_{1,i}}. \quad (31)$$

By using (31) and the nature of the one-dimensional search method, the real value of $Z_i = \cos \Theta_{L,i} \cos \Phi_{L,i}$ follows the uniform distribution within the region of $[\hat{Z}_i - b_i, \hat{Z}_i + b_i]$, where $b_i = \frac{\lambda_c}{2N_y d_1 S_{1,i}}$. The PDF of Z_i is thus given by

$$f_{Z_i}(z_i) = \begin{cases} \frac{1}{2b_i}, & \hat{Z}_i - b_i \leq z_i \leq \hat{Z}_i + b_i \\ 0, & \text{others.} \end{cases} \quad (32)$$

By denoting the estimation error of Z_i as \tilde{Z}_i , we have $\hat{Z}_i = Z_i + \tilde{Z}_i$. Then, the distribution of \tilde{Z}_i is given by

$$f_{\tilde{Z}_i}(\tilde{z}_i) = \begin{cases} \frac{1}{2b_i}, & -b_i \leq \tilde{z}_i \leq b_i \\ 0, & \text{others.} \end{cases} \quad (33)$$

Next, for simplicity, let us denote $U_i = \cos \Theta_{L,i}$. Then, by utilizing the definition of Z_i below (31) and X_i above (24), we have $Z_i = U_i X_i$. By combining the PDF of X_i in (30) and the PDF of Z_i in (32), we could derive the PDF of U_i as follows

$$f_{U_i}(u_i) = \int_{\hat{X}_i - \frac{\hat{Y}_i}{\hat{X}_i} a_i}^{\hat{X}_i + \frac{\hat{Y}_i}{\hat{X}_i} a_i} x f_{X_i}(x) f_{Z_i}(u_i x) dx. \quad (34)$$

According to (32), it is observed that $f_{Z_i}(u_i x)$ is non-zero when $\hat{Z}_i - b_i \leq u_i x \leq \hat{Z}_i + b_i$, which determines the PDF of U_i . Therefore, we need to discuss the different conditions according to the non-zero intervals of $f_{Z_i}(u_i x)$ and $f_{X_i}(x)$ in the following. For notation brevity, we denote $\alpha_{1,i} = \hat{X}_i - \frac{\hat{Y}_i}{\hat{X}_i} a_i$, $\alpha_{2,i} = \hat{X}_i + \frac{\hat{Y}_i}{\hat{X}_i} a_i$, $\beta_{1,i} = \hat{Z}_i - b_i$ and $\beta_{2,i} = \hat{Z}_i + b_i$.

Condition 1: If $\alpha_{1,i} < \frac{\beta_{1,i}}{u_i} \leq \alpha_{2,i} < \frac{\beta_{2,i}}{u_i}$, the integral interval of x in (34) can be recast as

$\left[\frac{\beta_{1,i}}{u_i}, \alpha_{2,i}\right]$, thereby yielding the PDF of U_i as

$$f_{U_i}(u_i) = \int_{\frac{\beta_{1,i}}{u_i}}^{\alpha_{2,i}} \frac{1}{2b_i} \cdot \frac{\hat{X}_i}{2a_i\hat{Y}_i} \cdot x dx = \frac{\hat{X}_i}{4a_i b_i \hat{Y}_i} \int_{\frac{\beta_{1,i}}{u_i}}^{\alpha_{2,i}} x dx = \frac{\hat{X}_i}{8a_i b_i \hat{Y}_i} \left(\alpha_{2,i}^2 - \left(\frac{\beta_{1,i}}{u_i} \right)^2 \right). \quad (35)$$

Furthermore, the interval of u_i is given by

$$\left[\frac{\beta_{1,i}}{\alpha_{2,i}}, \frac{\beta_{1,i}}{\alpha_{1,i}} \right) \cap \left(-\infty, \frac{\beta_{2,i}}{\alpha_{2,i}} \right). \quad (36)$$

Based on (36), it is necessary to compare $\frac{\beta_{1,i}}{\alpha_{1,i}}$ with $\frac{\beta_{2,i}}{\alpha_{2,i}}$, so that the interval of u_i can be further determined. If $\frac{\beta_{2,i}}{\alpha_{2,i}} > \frac{\beta_{1,i}}{\alpha_{1,i}}$ holds, the interval can be rewritten as $\left[\frac{\beta_{1,i}}{\alpha_{2,i}}, \frac{\beta_{1,i}}{\alpha_{1,i}} \right)$. Otherwise, the interval is $\left[\frac{\beta_{1,i}}{\alpha_{2,i}}, \frac{\beta_{2,i}}{\alpha_{2,i}} \right)$.

Condition 2: If $\frac{\beta_{1,i}}{u_i} \leq \alpha_{1,i} < \frac{\beta_{2,i}}{u_i} \leq \alpha_{2,i}$, the integral interval of x in (34) can be recast as $\left[\alpha_{1,i}, \frac{\beta_{2,i}}{u_i} \right]$, thus the PDF of U_i is given by

$$f_{U_i}(u_i) = \int_{\alpha_{1,i}}^{\frac{\beta_{2,i}}{u_i}} \frac{1}{2b_i} \cdot \frac{\hat{X}_i}{2a_i\hat{Y}_i} \cdot x dx = \frac{\hat{X}_i}{4a_i b_i \hat{Y}_i} \int_{\alpha_{1,i}}^{\frac{\beta_{2,i}}{u_i}} x dx = \frac{\hat{X}_i}{8a_i b_i \hat{Y}_i} \left(\left(\frac{\beta_{2,i}}{u_i} \right)^2 - \alpha_{1,i}^2 \right). \quad (37)$$

The interval of u_i is given by

$$\left[\frac{\beta_{2,i}}{\alpha_{2,i}}, \frac{\beta_{2,i}}{\alpha_{1,i}} \right) \cap \left[\frac{\beta_{1,i}}{\alpha_{1,i}}, +\infty \right). \quad (38)$$

As a result, if $\frac{\beta_{2,i}}{\alpha_{2,i}} > \frac{\beta_{1,i}}{\alpha_{1,i}}$ holds, the interval can be further recast as $\left[\frac{\beta_{2,i}}{\alpha_{2,i}}, \frac{\beta_{2,i}}{\alpha_{1,i}} \right)$. Otherwise, the interval can be derived as $\left[\frac{\beta_{1,i}}{\alpha_{1,i}}, \frac{\beta_{2,i}}{\alpha_{1,i}} \right)$.

Condition 3: If $\frac{\beta_{1,i}}{u_i} \leq \alpha_{1,i} < \alpha_{2,i} < \frac{\beta_{2,i}}{u_i}$, the integral interval of x in (34) can be derived as $[\alpha_{1,i}, \alpha_{2,i}]$. Thus, the PDF of U_i is

$$\begin{aligned} f_{U_i}(u_i) &= \int_{\alpha_{1,i}}^{\alpha_{2,i}} \frac{1}{2b_i} \cdot \frac{\hat{X}_i}{2a_i\hat{Y}_i} \cdot x dx = \frac{\hat{X}_i}{4a_i b_i \hat{Y}_i} \int_{\alpha_{1,i}}^{\alpha_{2,i}} x dx = \frac{\hat{X}_i}{8a_i b_i \hat{Y}_i} (\alpha_{2,i}^2 - \alpha_{1,i}^2) \\ &= \frac{\hat{X}_i}{8a_i b_i \hat{Y}_i} \left(\left(\hat{X}_i + \frac{\hat{Y}_i}{\hat{X}_i} a_i \right)^2 - \left(\hat{X}_i - \frac{\hat{Y}_i}{\hat{X}_i} a_i \right)^2 \right) = \frac{\hat{X}_i}{2b_i}. \end{aligned} \quad (39)$$

The interval of u_i is accordingly given by $\left[\frac{\beta_{1,i}}{\alpha_{1,i}}, \frac{\beta_{2,i}}{\alpha_{2,i}} \right)$.

Condition 4: If $\alpha_{1,i} < \frac{\beta_{1,i}}{u_i} < \frac{\beta_{2,i}}{u_i} \leq \alpha_{2,i}$, the integral interval of x in (34) can be derived as

$\left[\frac{\beta_{1,i}}{u_i}, \frac{\beta_{2,i}}{u_i}\right]$. Thus, the PDF of U_i is

$$f_{U_i}(u_i) = \int_{\frac{\beta_{1,i}}{u_i}}^{\frac{\beta_{2,i}}{u_i}} \frac{\hat{X}_i}{4a_i b_i \hat{Y}_i} \cdot x dx = \frac{\hat{X}_i}{4a_i b_i \hat{Y}_i} \int_{\frac{\beta_{1,i}}{u_i}}^{\frac{\beta_{2,i}}{u_i}} x dx = \frac{\hat{X}_i}{8a_i b_i \hat{Y}_i} \left(\left(\frac{\beta_{2,i}}{u_i} \right)^2 - \left(\frac{\beta_{1,i}}{u_i} \right)^2 \right) = \frac{\hat{X}_i \hat{Z}_i}{2a_i \hat{Y}_i u_i^2}. \quad (40)$$

Additionally, after some mathematical manipulations, we can derive the interval of u_i as $\left[\frac{\beta_{2,i}}{\alpha_{2,i}}, \frac{\beta_{1,i}}{\alpha_{1,i}}\right]$.

Based on the above discussions, by comparing $\frac{\beta_{2,i}}{\alpha_{2,i}}$ with $\frac{\beta_{1,i}}{\alpha_{1,i}}$, the PDF of U_i can be simplified as the following two cases:

Case 1: If $\frac{\beta_{2,i}}{\alpha_{2,i}} > \frac{\beta_{1,i}}{\alpha_{1,i}}$ holds, the intervals of u in Condition 1 and Condition 2 are given by $\left[\frac{\beta_{1,i}}{\alpha_{2,i}}, \frac{\beta_{1,i}}{\alpha_{1,i}}\right)$ and $\left[\frac{\beta_{2,i}}{\alpha_{2,i}}, \frac{\beta_{2,i}}{\alpha_{1,i}}\right)$. Additionally, Condition 3 is valid, whereas Condition 4 is invalid. Therefore, the PDF of U_i is written as

$$f_{U_i}(u_i) = \begin{cases} \frac{\hat{X}_i}{8a_i b_i \hat{Y}_i} \left(\alpha_{2,i}^2 - \left(\frac{\beta_{1,i}}{u_i} \right)^2 \right), & \frac{\beta_{1,i}}{\alpha_{2,i}} \leq u_i < \frac{\beta_{1,i}}{\alpha_{1,i}} \\ \frac{\hat{X}_i}{2b_i}, & \frac{\beta_{1,i}}{\alpha_{1,i}} \leq u_i < \frac{\beta_{2,i}}{\alpha_{2,i}} \\ \frac{\hat{X}_i}{8a_i b_i \hat{Y}_i} \left(\left(\frac{\beta_{2,i}}{u_i} \right)^2 - \alpha_{1,i}^2 \right), & \frac{\beta_{2,i}}{\alpha_{2,i}} \leq u_i \leq \frac{\beta_{2,i}}{\alpha_{1,i}} \\ 0, & \text{others.} \end{cases} \quad (41)$$

Case 2: If $\frac{\beta_{2,i}}{\alpha_{2,i}} < \frac{\beta_{1,i}}{\alpha_{1,i}}$ holds, the intervals of u_i in Condition 1 and Condition 2 are given by $\left[\frac{\beta_{1,i}}{\alpha_{2,i}}, \frac{\beta_{2,i}}{\alpha_{2,i}}\right)$ and $\left[\frac{\beta_{1,i}}{\alpha_{1,i}}, \frac{\beta_{2,i}}{\alpha_{1,i}}\right)$, respectively. Moreover, Condition 4 is valid, while Condition 3 is invalid. Accordingly, the PDF of U_i can be derived as

$$f_{U_i}(u_i) = \begin{cases} \frac{\hat{X}_i}{8a_i b_i \hat{Y}_i} \left(\alpha_{2,i}^2 - \left(\frac{\beta_{1,i}}{u_i} \right)^2 \right), & \frac{\beta_{1,i}}{\alpha_{2,i}} \leq u_i < \frac{\beta_{2,i}}{\alpha_{2,i}} \\ \frac{\hat{X}_i \hat{Z}_i}{2a_i \hat{Y}_i u_i^2}, & \frac{\beta_{2,i}}{\alpha_{2,i}} \leq u_i < \frac{\beta_{1,i}}{\alpha_{1,i}} \\ \frac{\hat{X}_i}{8a_i b_i \hat{Y}_i} \left(\left(\frac{\beta_{2,i}}{u_i} \right)^2 - \alpha_{1,i}^2 \right), & \frac{\beta_{1,i}}{\alpha_{1,i}} \leq u_i \leq \frac{\beta_{2,i}}{\alpha_{1,i}} \\ 0, & \text{others.} \end{cases} \quad (42)$$

3) *PDF of $\Theta_{L,i}$* : By using the PDF of $\cos \Theta_{L,i}$, the PDF of $\Theta_{L,i}$ can be derived as follows.

First of all, the CDF of $\Theta_{L,i}$ can be derived as follows

$$F_{\Theta_{L,i}}(\theta_{L,i}) = \Pr(\Theta_{L,i} \leq \theta_{L,i}) = \Pr(\arccos U_i \leq \theta_{L,i}) = 1 - \Pr(U_i \leq \cos \theta_{L,i}). \quad (43)$$

Then, the PDF of $\Theta_{L,i}$ is obtained as follows

$$f_{\Theta_{L,i}}(\theta_{L,i}) = \frac{\partial F_{\Theta_{L,i}}(\theta_{L,i})}{\partial \theta_{L,i}} = \sin \theta_{L,i} f_{U_i}(\cos \theta_{L,i}). \quad (44)$$

Furthermore, we consider the indoor positioning system in this paper, where the RISs are supposed to be mounted on the wall. Hence we have $\Theta_{L,i} \in (0, \pi)$. Thus, $\Theta_{L,i}$ decreases monotonically with U_i . According to the PDF of U_i in the aforementioned two cases, we can derive the PDF of $\Theta_{L,i}$ in the following.

Case 1: When $\frac{\beta_{2,i}}{\alpha_{2,i}} > \frac{\beta_{1,i}}{\alpha_{1,i}}$, according to (41), we can derive the PDF of $\Theta_{L,i}$, which is given by

$$f_{\Theta_{L,i}}(\theta_{L,i}) = \begin{cases} \frac{\hat{X}_i \sin \theta_{L,i}}{8a_i b_i \hat{Y}_i} \left[\left(\frac{\beta_{2,i}}{\cos \theta_{L,i}} \right)^2 - \alpha_{1,i}^2 \right], & \arccos \frac{\beta_{2,i}}{\alpha_{1,i}} \leq \theta_{L,i} \leq \arccos \frac{\beta_{2,i}}{\alpha_{2,i}} \\ \frac{\hat{X}_i \sin \theta_{L,i}}{2b_i}, & \arccos \frac{\beta_{2,i}}{\alpha_{2,i}} < \theta_{L,i} \leq \arccos \frac{\beta_{1,i}}{\alpha_{1,i}} \\ \frac{\hat{X}_i \sin \theta_{L,i}}{8a_i b_i \hat{Y}_i} \left[\alpha_{2,i}^2 - \left(\frac{\beta_{1,i}}{\cos \theta_{L,i}} \right)^2 \right], & \arccos \frac{\beta_{1,i}}{\alpha_{1,i}} < \theta_{L,i} \leq \arccos \frac{\beta_{1,i}}{\alpha_{2,i}} \\ 0, & \text{others.} \end{cases} \quad (45)$$

Case 2: When $\frac{\beta_{2,i}}{\alpha_{2,i}} < \frac{\beta_{1,i}}{\alpha_{1,i}}$, we can derive the PDF of $\Theta_{L,i}$ based on (42), which is given by

$$f_{\Theta_{L,i}}(\theta_{L,i}) = \begin{cases} \frac{\hat{X}_i \sin \theta_{L,i}}{8a_i b_i \hat{Y}_i} \left[\left(\frac{\beta_{2,i}}{\cos \theta_{L,i}} \right)^2 - \alpha_{1,i}^2 \right], & \arccos \frac{\beta_{2,i}}{\alpha_{1,i}} \leq \theta_{L,i} \leq \arccos \frac{\beta_{1,i}}{\alpha_{1,i}} \\ \frac{\hat{X}_i \hat{Z}_i \sin \theta_{L,i}}{2a_i \hat{Y}_i (\cos \theta_{L,i})^2}, & \arccos \frac{\beta_{1,i}}{\alpha_{1,i}} \leq \theta_{L,i} < \arccos \frac{\beta_{2,i}}{\alpha_{2,i}} \\ \frac{\hat{X}_i \sin \theta_{L,i}}{8a_i b_i \hat{Y}_i} \left[\alpha_{2,i}^2 - \left(\frac{\beta_{1,i}}{\cos \theta_{L,i}} \right)^2 \right], & \arccos \frac{\beta_{2,i}}{\alpha_{2,i}} \leq \theta_{L,i} < \arccos \frac{\beta_{1,i}}{\alpha_{2,i}} \\ 0, & \text{others.} \end{cases} \quad (46)$$

4) *PDF of $\tilde{\Theta}_{L,i}$* : By using the CDF and PDF of $\Theta_{L,i}$ in (43), (45) and (46), we can calculate the CDF and PDF of $\tilde{\Theta}_{L,i}$ as follows.

Firstly, based on $\hat{\Theta}_{L,i} = \Theta_{L,i} + \tilde{\Theta}_{L,i}$, the CDF of $\tilde{\Theta}_{L,i}$ can be derived as follows

$$\begin{aligned} F_{\tilde{\Theta}_{L,i}}(\tilde{\theta}_{L,i}) &= \Pr(\tilde{\Theta}_{L,i} \leq \tilde{\theta}_{L,i}) = \Pr(\hat{\Theta}_{L,i} - \Theta_{L,i} \leq \tilde{\theta}_{L,i}) \\ &= \Pr(\Theta_{L,i} \geq \hat{\Theta}_{L,i} - \tilde{\theta}_{L,i}) = 1 - \Pr(\Theta_{L,i} \leq \hat{\Theta}_{L,i} - \tilde{\theta}_{L,i}). \end{aligned} \quad (47)$$

Then, based on the above two cases of $f_{\Theta_{L,i}}(\theta_{L,i})$ in (45) and (46), the PDF of $\tilde{\Theta}_{L,i}$ can be derived accordingly by using (47).

Case 1: When $\frac{\beta_{2,i}}{\alpha_{2,i}} > \frac{\beta_{1,i}}{\alpha_{1,i}}$, by using (45), the PDF of $\tilde{\Theta}_{L,i}$ is calculated as

$$f_{\tilde{\Theta}_{L,i}}(\tilde{\theta}_{L,i}) = \frac{\partial F_{\tilde{\Theta}_{L,i}}(\tilde{\theta}_{L,i})}{\partial \tilde{\theta}_{L,i}} = f_{\Theta_{L,i}}(\hat{\Theta}_{L,i} - \tilde{\theta}_{L,i})$$

$$= \begin{cases} \frac{\hat{X}_i \sin(\hat{\Theta}_{L,i} - \tilde{\theta}_{L,i})}{8a_i b_i \hat{Y}_i} \left[\alpha_{2,i}^2 - \left(\frac{\beta_{1,i}}{\cos(\hat{\Theta}_{L,i} - \tilde{\theta}_{L,i})} \right)^2 \right], & \hat{\Theta}_{L,i} - \arccos \frac{\beta_{1,i}}{\alpha_{2,i}} \leq \tilde{\theta}_{L,i} < \hat{\Theta}_{L,i} - \arccos \frac{\beta_{1,i}}{\alpha_{1,i}} \\ \frac{\hat{X}_i \sin(\hat{\Theta}_{L,i} - \tilde{\theta}_{L,i})}{8a_i b_i \hat{Y}_i} \left[\frac{\hat{X}_i \sin(\hat{\Theta}_{L,i} - \tilde{\theta}_{L,i})}{2b_i} \right], & \hat{\Theta}_{L,i} - \arccos \frac{\beta_{1,i}}{\alpha_{1,i}} \leq \tilde{\theta}_{L,i} < \hat{\Theta}_{L,i} - \arccos \frac{\beta_{2,i}}{\alpha_{2,i}} \\ \frac{\hat{X}_i \sin(\hat{\Theta}_{L,i} - \tilde{\theta}_{L,i})}{8a_i b_i \hat{Y}_i} \left[\left(\frac{\beta_{2,i}}{\cos(\hat{\Theta}_{L,i} - \tilde{\theta}_{L,i})} \right)^2 - \alpha_{1,i}^2 \right], & \hat{\Theta}_{L,i} - \arccos \frac{\beta_{2,i}}{\alpha_{2,i}} \leq \tilde{\theta}_{L,i} \leq \hat{\Theta}_{L,i} - \arccos \frac{\beta_{2,i}}{\alpha_{1,i}} \\ 0, & \text{others.} \end{cases} \quad (48)$$

Case 2: When $\frac{\beta_{2,i}}{\alpha_{2,i}} < \frac{\beta_{1,i}}{\alpha_{1,i}}$, we can derive the PDF of $\tilde{\Theta}_{L,i}$ by using (46), which is given by

$$f_{\tilde{\Theta}_{L,i}}(\tilde{\theta}_{L,i}) = \frac{\partial F_{\tilde{\Theta}_{L,i}}(\tilde{\theta}_{L,i})}{\partial \tilde{\theta}_{L,i}} = f_{\Theta_{L,i}}(\hat{\Theta}_{L,i} - \tilde{\theta}_{L,i})$$

$$= \begin{cases} \frac{\hat{X}_i \sin(\hat{\Theta}_{L,i} - \tilde{\theta}_{L,i})}{8a_i b_i \hat{Y}_i} \left(\alpha_{2,i}^2 - \left(\frac{\beta_{1,i}}{\cos(\hat{\Theta}_{L,i} - \tilde{\theta}_{L,i})} \right)^2 \right), & \hat{\Theta}_{L,i} - \arccos \frac{\beta_{1,i}}{\alpha_{2,i}} \leq \tilde{\theta}_{L,i} < \hat{\Theta}_{L,i} - \arccos \frac{\beta_{2,i}}{\alpha_{2,i}} \\ \frac{\hat{X}_i \hat{Z}_i \sin(\hat{\Theta}_{L,i} - \tilde{\theta}_{L,i})}{2a_i \hat{Y}_i [\cos(\hat{\Theta}_{L,i} - \tilde{\theta}_{L,i})]^2}, & \hat{\Theta}_{L,i} - \arccos \frac{\beta_{2,i}}{\alpha_{2,i}} \leq \tilde{\theta}_{L,i} < \hat{\Theta}_{L,i} - \arccos \frac{\beta_{1,i}}{\alpha_{1,i}} \\ \frac{\hat{X}_i \sin(\hat{\Theta}_{L,i} - \tilde{\theta}_{L,i})}{8a_i b_i \hat{Y}_i} \left[\left(\frac{\beta_{2,i}}{\cos(\hat{\Theta}_{L,i} - \tilde{\theta}_{L,i})} \right)^2 - \alpha_{1,i}^2 \right], & \hat{\Theta}_{L,i} - \arccos \frac{\beta_{1,i}}{\alpha_{1,i}} \leq \tilde{\theta}_{L,i} \leq \hat{\Theta}_{L,i} - \arccos \frac{\beta_{2,i}}{\alpha_{1,i}} \\ 0, & \text{others.} \end{cases} \quad (49)$$

To facilitate the error analysis, we now aim to derive the approximation of $f_{\tilde{\Theta}_{L,i}}(\tilde{\theta}_{L,i})$ in this paper. As we have assumed that the estimation error is very small, we have $\sin \tilde{\theta}_{L,i} \approx \tilde{\theta}_{L,i}$ and $\cos \tilde{\theta}_{L,i} \approx 1$, leading to

$$\begin{aligned} \sin(\hat{\Theta}_{L,i} - \tilde{\theta}_{L,i}) &= \sin \hat{\Theta}_{L,i} \cos \tilde{\theta}_{L,i} - \sin \tilde{\theta}_{L,i} \cos \hat{\Theta}_{L,i} \approx \sin \hat{\Theta}_{L,i} - \tilde{\theta}_{L,i} \cos \hat{\Theta}_{L,i}, \\ \cos(\hat{\Theta}_{L,i} - \tilde{\theta}_{L,i}) &= \cos \hat{\Theta}_{L,i} \cos \tilde{\theta}_{L,i} + \sin \hat{\Theta}_{L,i} \sin \tilde{\theta}_{L,i} \approx \cos \hat{\Theta}_{L,i} + \tilde{\theta}_{L,i} \sin \hat{\Theta}_{L,i}. \end{aligned} \quad (50)$$

Using the approximations in (50), we can derive the approximation of $f_{\tilde{\Theta}_{L,i}}(\tilde{\theta}_{L,i})$ according to the above two cases. Furthermore, by denoting $\sin \hat{\Theta}_{L,i} = \hat{V}_i$, $\cos \hat{\Theta}_{L,i} = \hat{U}_i$, $B_{1,i} = \hat{\Theta}_{L,i} - \arccos \frac{\beta_{1,i}}{\alpha_{2,i}}$, $B_{2,i} = \hat{\Theta}_{L,i} - \arccos \frac{\beta_{1,i}}{\alpha_{1,i}}$, $B_{3,i} = \hat{\Theta}_{L,i} - \arccos \frac{\beta_{2,i}}{\alpha_{2,i}}$, $B_{4,i} = \hat{\Theta}_{L,i} - \arccos \frac{\beta_{2,i}}{\alpha_{1,i}}$, the expression could be further simplified in the following.

Case 1: When $\frac{\beta_{2,i}}{\alpha_{2,i}} > \frac{\beta_{1,i}}{\alpha_{1,i}}$, based on (48), we can derive the approximation of $f_{\tilde{\Theta}_{L,i}}(\tilde{\theta}_{L,i})$,

which is written as

$$f_{\tilde{\Theta}_{L,i}}(\tilde{\theta}_{L,i}) \approx \begin{cases} \frac{\hat{X}_i(\hat{V}_i - \tilde{\theta}_{L,i}\hat{U}_i)}{8a_i b_i \hat{Y}_i} \left[\alpha_{2,i}^2 - \left(\frac{\beta_{1,i}}{\hat{U}_i + \tilde{\theta}_{L,i}\hat{V}_i} \right)^2 \right], & B_{1,i} \leq \tilde{\theta}_{L,i} < B_{2,i} \\ \frac{\hat{X}_i(\hat{V}_i - \tilde{\theta}_{L,i}\hat{U}_i)}{2b_i}, & B_{2,i} \leq \tilde{\theta}_{L,i} < B_{3,i} \\ \frac{\hat{X}_i(\hat{V}_i - \tilde{\theta}_{L,i}\hat{U}_i)}{8a_i b_i \hat{Y}_i} \left[\left(\frac{\beta_{2,i}}{\hat{U}_i + \tilde{\theta}_{L,i}\hat{V}_i} \right)^2 - \alpha_{1,i}^2 \right], & B_{3,i} \leq \tilde{\theta}_{L,i} \leq B_{4,i} \\ 0, & \text{others.} \end{cases} \quad (51)$$

Case 2: When $\frac{\beta_{2,i}}{\alpha_{2,i}} < \frac{\beta_{1,i}}{\alpha_{1,i}}$, as we have (49), we could derive the approximation of $f_{\tilde{\Theta}_{L,i}}(\tilde{\theta}_{L,i})$, which is written as

$$f_{\tilde{\theta}_{L,i}}(\tilde{\theta}_{L,i}) \approx \begin{cases} \frac{\hat{X}_i(\hat{V}_i - \tilde{\theta}_{L,i}\hat{U}_i)}{8a_i b_i \hat{Y}_i} \left[\alpha_{2,i}^2 - \left(\frac{\beta_{1,i}}{\hat{U}_i + \tilde{\theta}_{L,i}\hat{V}_i} \right)^2 \right], & B_{1,i} \leq \tilde{\theta}_{L,i} < B_{3,i} \\ \frac{\hat{X}_i \hat{Z}_i (\hat{V}_i - \tilde{\theta}_{L,i}\hat{U}_i)}{2a \hat{Y}_i (\hat{U}_i + \tilde{\theta}_{L,i}\hat{V}_i)^2}, & B_{3,i} \leq \tilde{\theta}_{L,i} < B_{2,i} \\ \frac{\hat{X}_i(\hat{V}_i - \tilde{\theta}_{L,i}\hat{U}_i)}{8a_i b_i \hat{Y}_i} \left[\left(\frac{\beta_{2,i}}{\hat{U}_i + \tilde{\theta}_{L,i}\hat{V}_i} \right)^2 - \alpha_{1,i}^2 \right], & B_{2,i} \leq \tilde{\theta}_{L,i} \leq B_{4,i} \\ 0, & \text{others.} \end{cases} \quad (52)$$

VI. VARIANCE OF ANGLE ESTIMATION ERROR

In this section, we aim to calculate the variance of $\tilde{\Phi}_{L,i}$ and $\tilde{\Theta}_{L,i}$ by using the PDF in the above section, which will be used for the 3D position estimation in the next section.

A. Variance of $\tilde{\Phi}_{L,i}$

In this subsection, we provide the variance expression of $\tilde{\Phi}_{L,i}$. Based on the PDF of $\tilde{\Phi}_{L,i}$ in (23), the variance of $\tilde{\Phi}_{L,i}$ can be calculated as

$$\begin{aligned} D(\tilde{\phi}_{L,i}) &= E(\tilde{\phi}_{L,i}^2) - (E(\tilde{\phi}_{L,i}))^2 \\ &= \int_{\hat{\Phi}_{L,i}-a_{1,i}}^{\hat{\Phi}_{L,i}-a_{2,i}} \tilde{\phi}_{L,i}^2 f_{\tilde{\Phi}_{L,i}}(\tilde{\phi}_{L,i}) d\tilde{\phi}_{L,i} - \left(\int_{\hat{\Phi}_{L,i}-a_{1,i}}^{\hat{\Phi}_{L,i}-a_{2,i}} \tilde{\phi}_{L,i} f_{\tilde{\Phi}_{L,i}}(\tilde{\phi}_{L,i}) d\tilde{\phi}_{L,i} \right)^2 \\ &= \frac{1}{2a_i} \left(\frac{\tilde{\phi}_{L,i}^3}{3} \cos \hat{\Phi}_{L,i} + \frac{\tilde{\phi}_{L,i}^4}{4} \sin \hat{\Phi}_{L,i} \right) \Big|_{\hat{\Phi}_{L,i}-a_{1,i}}^{\hat{\Phi}_{L,i}-a_{2,i}} \\ &\quad - \frac{1}{4a_i^2} \left[\left(\frac{\tilde{\phi}_{L,i}^2}{2} \cos \hat{\Phi}_{L,i} + \frac{\tilde{\phi}_{L,i}^3}{3} \sin \hat{\Phi}_{L,i} \right) \Big|_{\hat{\Phi}_{L,i}-a_{1,i}}^{\hat{\Phi}_{L,i}-a_{2,i}} \right]^2, \end{aligned} \quad (53)$$

where $f(x) \Big|_{x_2}^{x_1} = f(x_1) - f(x_2)$ and $E(\tilde{\phi}_{L,i})$ denotes the expectation of $\tilde{\phi}_{L,i}$.

B. Variance of $\tilde{\Theta}_{L,i}$

In this subsection, we aim to derive the variance of $\tilde{\Theta}_{L,i}$. Different from the PDF of $\tilde{\Phi}_{L,i}$, the PDF of $\tilde{\Theta}_{L,i}$ is more complicated. Therefore, we need to analyze the variance according to the aforementioned two cases as follows.

Case 1: When $\frac{\beta_{2,i}}{\alpha_{2,i}} > \frac{\beta_{1,i}}{\alpha_{1,i}}$, based on the PDF of $\tilde{\theta}_{L,i}$ in (51), the variance of $\tilde{\Theta}_{L,i}$ is derived as

$$D(\tilde{\theta}_{L,i}) = \underbrace{\int \tilde{\theta}_{L,i}^2 f_{\tilde{\Theta}_{L,i}}(\tilde{\theta}_{L,i}) d\tilde{\theta}_{L,i}}_{D_{1,i}} - \left(\underbrace{\int \tilde{\theta}_{L,i} f_{\tilde{\Theta}_{L,i}}(\tilde{\theta}_{L,i}) d\tilde{\theta}_{L,i}}_{D_{2,i}} \right)^2. \quad (54)$$

For $D_{1,i}$ in (54), we divide it into three different non-zero intervals that can be expressed as

$$D_{1,i} = D_{11,i} + D_{12,i} + D_{13,i}, \quad (55)$$

where $D_{11,i}$, $D_{12,i}$ and $D_{13,i}$ are the integral expressions in the intervals of $[B_{1,i}, B_{2,i})$, $[B_{2,i}, B_{3,i})$ and $[B_{3,i}, B_{4,i}]$, respectively. The expressions of $D_{11,i}$, $D_{12,i}$ and $D_{13,i}$ are given in Appendix A.

For $D_{2,i}$ in (54), it is the expectation of $\tilde{\theta}_{L,i}$, which is denoted by $E(\tilde{\theta}_{L,i})$. It can be divided into three different non-zero intervals that are given by

$$D_{2,i} = D_{21,i} + D_{22,i} + D_{23,i}, \quad (56)$$

where $D_{21,i}$, $D_{22,i}$ and $D_{23,i}$ are the integral expressions in the intervals of $[B_{1,i}, B_{2,i})$, $[B_{2,i}, B_{3,i})$ and $[B_{3,i}, B_{4,i}]$, respectively. The expressions of $D_{21,i}$, $D_{22,i}$ and $D_{23,i}$ are given in Appendix B.

Case 2: When $\frac{\beta_{2,i}}{\alpha_{2,i}} < \frac{\beta_{1,i}}{\alpha_{1,i}}$, according to the PDF of $\tilde{\Theta}_{L,i}$ in (52), the variance of $\tilde{\Theta}_{L,i}$ can be calculated as

$$D'(\tilde{\theta}_{L,i}) = \underbrace{\int \tilde{\theta}_{L,i}^2 f_{\tilde{\Theta}_{L,i}}(\tilde{\theta}_{L,i}) d\tilde{\theta}_{L,i}}_{D'_{1,i}} - \left(\underbrace{\int \tilde{\theta}_{L,i} f_{\tilde{\Theta}_{L,i}}(\tilde{\theta}_{L,i}) d\tilde{\theta}_{L,i}}_{D'_{2,i}} \right)^2. \quad (57)$$

For $D'_{1,i}$, we divide it into three different non-zero intervals that are given by

$$D'_{1,i} = D'_{11,i} + D'_{12,i} + D'_{13,i}, \quad (58)$$

where $D'_{11,i}$, $D'_{12,i}$ and $D'_{13,i}$ are the integral expressions in the intervals of $[B_{1,i}, B_{3,i})$, $[B_{3,i}, B_{2,i})$ and $[B_{2,i}, B_{4,i}]$. The expressions of $D'_{11,i}$, $D'_{12,i}$ and $D'_{13,i}$ are given in Appendix C.

For $D'_{2,i}$ in (57), it is the expectation of $\tilde{\theta}_{L,i}$, which is denoted by $E(\tilde{\theta}_{L,i})$. It is also divided

into three different non-zero intervals that are given by

$$D'_{2,i} = D'_{21,i} + D'_{22,i} + D'_{23,i}, \quad (59)$$

where $D'_{21,i}$, $D'_{22,i}$ and $D'_{23,i}$ are the integral expressions in the intervals of $[B_{1,i}, B_{3,i})$, $[B_{3,i}, B_{2,i})$ and $[B_{2,i}, B_{4,i}]$. The expressions of $D'_{21,i}$, $D'_{22,i}$ and $D'_{23,i}$ are given in Appendix D.

VII. 3D POSITION ESTIMATION

Using the estimated AoA in Section IV and the variance of the estimation error in Section VI, we aim to derive the expression of the estimation of the MU's 3D position at this section. First, we have the AoAs at the i th anchor given by

$$\begin{aligned} \hat{\Theta}_{L,i} &= \Theta_{L,i} + \tilde{\Theta}_{L,i} \\ \hat{\Phi}_{L,i} &= \Phi_{L,i} + \tilde{\Phi}_{L,i}, \end{aligned} \quad (60)$$

where $\hat{\Theta}_{L,i}$ and $\hat{\Phi}_{L,i}$ denote the estimated AoAs at the i th anchor, $\Theta_{L,i}$ and $\Phi_{L,i}$ denote the true AoAs at the i th anchor, and $\tilde{\Theta}_{L,i}$ and $\tilde{\Phi}_{L,i}$ denote the estimation error at the i th anchor. For the sake of illustration, we collect all the estimated AoAs in the following vectors:

$$\begin{aligned} \hat{\Theta} &= \Theta + \tilde{\Theta}, \\ \hat{\Phi} &= \Phi + \tilde{\Phi}, \end{aligned} \quad (61)$$

where

$$\begin{aligned} \hat{\Theta} &= [\hat{\Theta}_{L,1}, \dots, \hat{\Theta}_{L,I}], & \hat{\Phi} &= [\hat{\Phi}_{L,1}, \dots, \hat{\Phi}_{L,I}], \\ \Theta &= [\Theta_{L,1}, \dots, \Theta_{L,I}], & \Phi &= [\Phi_{L,1}, \dots, \Phi_{L,I}], \\ \tilde{\Theta} &= [\tilde{\Theta}_{L,1}, \dots, \tilde{\Theta}_{L,I}], & \tilde{\Phi} &= [\tilde{\Phi}_{L,1}, \dots, \tilde{\Phi}_{L,I}]. \end{aligned} \quad (62)$$

In the existing works, for tractability, $\tilde{\Theta}$ and $\tilde{\Phi}$ are assumed to be the additive complex Gaussian noise with zero mean. However, according to the angle estimation error analysis in our previous section, the PDF of the estimation error $\tilde{\Phi}$ should be modeled as (23), while the PDF of the estimation error $\tilde{\Theta}$ should be modeled as (51) or (52). Furthermore, the covariance

matrices can be written as

$$\begin{aligned}\mathbf{Q}_\Theta &= \text{diag}[\sigma_{\tilde{\Theta}_{L,1}}^2, \dots, \sigma_{\tilde{\Theta}_{L,I}}^2], \\ \mathbf{Q}_\Phi &= \text{diag}[\sigma_{\tilde{\Phi}_{L,1}}^2, \dots, \sigma_{\tilde{\Phi}_{L,I}}^2],\end{aligned}\quad (63)$$

where $\sigma_{\tilde{\Theta}_{L,i}}^2$ and $\sigma_{\tilde{\Phi}_{L,i}}^2$ denote the variance of $\tilde{\Theta}_{L,i}$ and $\tilde{\Phi}_{L,i}$, respectively. $\sigma_{\tilde{\Phi}_{L,i}}^2$ can be calculated according to (53), and $\sigma_{\tilde{\Theta}_{L,i}}^2$ can be calculated according to (54) or (57).

Accordingly, we propose to derive the closed-form expression of the MU's estimated 3D position. First, we can derive the pseudolinear equations [25] based on the estimated AoAs as follows:

$$\begin{aligned}\hat{\mathbf{g}}_{\Theta_i}^T \mathbf{s}_i - \hat{\mathbf{g}}_{\Theta_i}^T \mathbf{q} &\approx -\tilde{\Theta}_{L,i} d_{L,i} \cos \hat{\Phi}_{L,i}, \\ \hat{\mathbf{g}}_{\Phi_i}^T \mathbf{s}_i - \hat{\mathbf{g}}_{\Phi_i}^T \mathbf{q} &\approx -\tilde{\Theta}_{L,i} d_{L,i},\end{aligned}\quad (64)$$

where $d_{L,i}$ denotes the distance between the i th anchor and the MU, and we have

$$\hat{\mathbf{g}}_{\Theta_i} = [-\cos \hat{\Theta}_{L,i}, \sin \hat{\Theta}_{L,i}, 0]^T, \hat{\mathbf{g}}_{\Phi_i} = [-\sin \hat{\Phi}_{L,i} \sin \hat{\Theta}_{L,i}, \sin \hat{\Phi}_{L,i} \cos \hat{\Theta}_{L,i}, -\cos \hat{\Phi}_{L,i}]^T. \quad (65)$$

As a result, we can derive the following compact form of equations as

$$\hat{\mathbf{h}} - \hat{\mathbf{G}}\mathbf{q} = \mathbf{B}\mathbf{z} \quad (66)$$

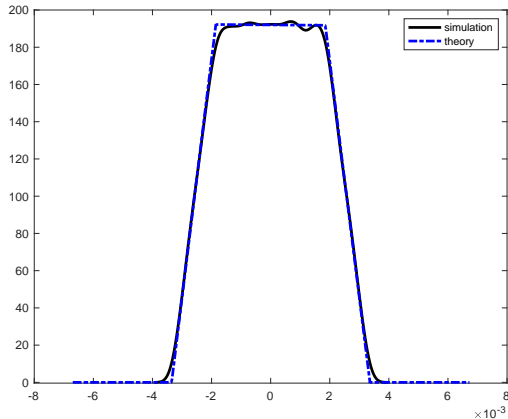
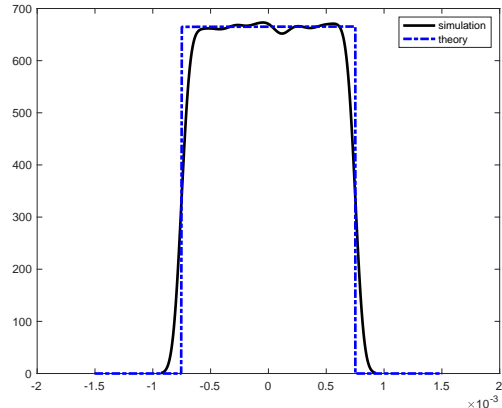
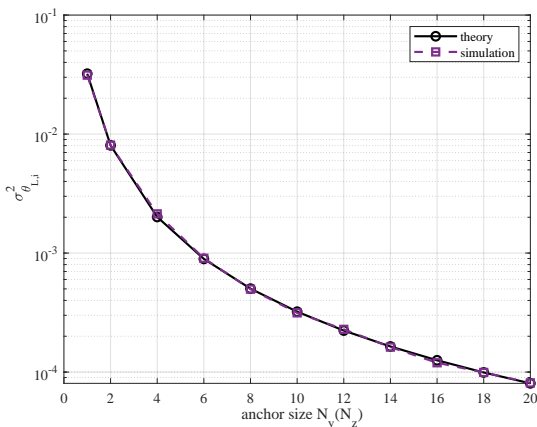
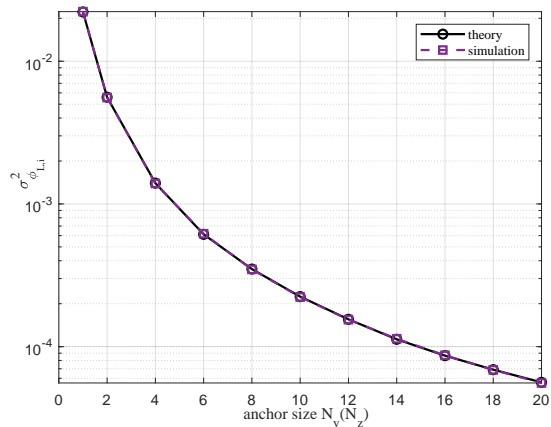
where

$$\begin{aligned}\hat{\mathbf{h}} &= [\mathbf{1}^T (\hat{\mathbf{G}}_\Theta \odot \mathbf{S})^T, \mathbf{1}^T (\hat{\mathbf{G}}_\Phi \odot \mathbf{S})^T]^T, \hat{\mathbf{G}} = [\hat{\mathbf{G}}_\Theta^T, \hat{\mathbf{G}}_\Phi^T]^T, \mathbf{B} = [\mathbf{B}_1, \mathbf{B}_2]^T, \mathbf{z} = [\tilde{\Theta}^T, \tilde{\Phi}^T]^T, \\ \hat{\mathbf{G}}_\Theta &= [\hat{\mathbf{g}}_{\Theta_1}, \dots, \hat{\mathbf{g}}_{\Theta_I}]^T, \hat{\mathbf{G}}_\Phi = [\hat{\mathbf{g}}_{\Phi_1}, \dots, \hat{\mathbf{g}}_{\Phi_I}]^T, \mathbf{S} = [\mathbf{s}_1, \dots, \mathbf{s}_I]^T, \mathbf{B}_1 = [\mathbf{B}_\Theta, \mathbf{O}]^T, \mathbf{B}_2 = [\mathbf{O}, \mathbf{B}_\Phi]^T, \\ \mathbf{B}_\Theta &= -\text{diag}[d_{L,1} \cos \hat{\Phi}_{L,1}, \dots, d_{L,I} \cos \hat{\Phi}_{L,I}]^T, \mathbf{B}_\Phi = -\text{diag}[d_{L,1}, \dots, d_{L,I}]^T.\end{aligned}\quad (67)$$

Based on (66), we can apply the WLS algorithm [25] to derive the closed-form expression of the MU's estimated position, which is written as:

$$\hat{\mathbf{q}} = (\hat{\mathbf{G}}^T \mathbf{W} \hat{\mathbf{G}})^{-1} \hat{\mathbf{G}}^T \mathbf{W} \hat{\mathbf{h}}, \quad (68)$$

where $\mathbf{W} = \mathbf{B}\mathbf{Q}\mathbf{B}^T$ and $\mathbf{Q} = \text{diag}[\mathbf{Q}_\Theta, \mathbf{Q}_\Phi]$. The details of the derivation can be found in [25].

Fig. 2: PDF of $\tilde{\Theta}_{L,i}$.Fig. 3: PDF of $\tilde{\Phi}_{L,i}$.Fig. 4: Variance of $\tilde{\Theta}_{L,i}$ versus anchor size.Fig. 5: Variance of $\tilde{\Phi}_{L,i}$ versus anchor size.

VIII. SIMULATION RESULTS

This section presents simulation results to validate the accuracy of our derivations and approximations. In our simulation, we consider a mmWave multiple input single output (MISO) channel from the MU to the anchors. Moreover, the MU, the anchors are assumed to be placed in a 3D area. The locations of four anchors are $\mathbf{s}_1 = [2, 20, 3]^T$, $\mathbf{s}_2 = [-12, -16, 58]^T$, $\mathbf{s}_3 = [-10, -6, -8]^T$ and $\mathbf{s}_4 = [10, 6, -20]^T$. It is assumed that the inter-antenna spacing of UPA at the anchors is $d_r = \lambda_c/2$. The following results are obtained by averaging over 10,000 random estimation error realizations. Unless otherwise stated, we assume $S = S_1 \times S_2 = 64 \times 64$ for rotation angle search grids, and the SNR is assumed to be 10 dB. The positioning accuracy is assessed in terms of the mean-square error (MSE).

Fig. 2 and Fig. 3 illustrate the PDF of estimation errors. It is assumed that the anchor size is $N_y = N_z = 16$. It can be observed from Fig. 2 and Fig. 3 that our derived results match well

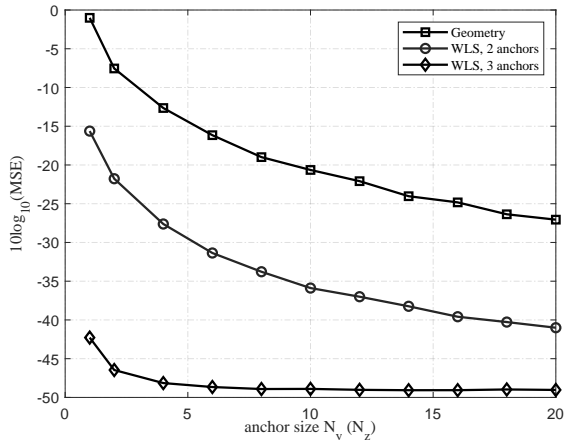


Fig. 6: Comparison of the proposed framework and geometry algorithm.

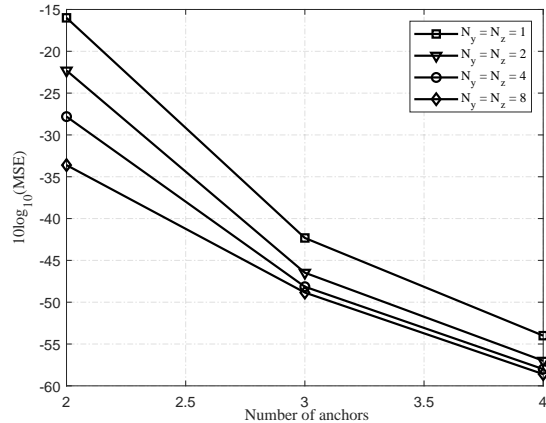


Fig. 7: MSE of the proposed framework versus anchors number.

with the simulation results, which verify the accuracy of our derived results and confirm that the angle estimation error is non-Gaussian.

Fig. 4 and Fig. 5 display the variance $\sigma_{\tilde{\Theta}_{L,i}}^2$ of estimation error $\tilde{\Theta}_{L,i}$ and the variance $\sigma_{\tilde{\Phi}_{L,i}}^2$ of estimation error $\tilde{\Phi}_{L,i}$ as the functions of anchor size $N_y(N_z)$, respectively. Fig. 4 and Fig. 5 display the variance $\sigma_{\tilde{\Theta}_{L,i}}^2$, which show that the theoretical results coincide with the simulation results, which validates the correctness of the derived results. Moreover, it is observed that the variances of $\tilde{\Theta}_{L,i}$ and $\tilde{\Phi}_{L,i}$ decrease with the anchor size, which means that increasing the number of antennas could improve the estimation accuracy.

Fig. 6 compares the MSE of the proposed framework aided by 2 anchors with that aided by 3 anchors when the size of anchors increases from $N_y = N_z = 1$ to $N_y = N_z = 20$. As shown in the figure, the MSE decreases with the anchor size as expected. Furthermore, it is shown that the MSE of 2 anchors is larger than that of 3 anchors. It implies that increasing the number of anchors can significantly improve the positioning accuracy of the proposed framework.

In [26], the position of the MU is derived by using the geometry relationship between the estimated AOA and the 3D position, which is denoted as the geometry algorithm in this paper. Fig. 6 also presents the positioning performance comparison of the proposed framework with the geometry algorithm. It is seen from Fig. 6 that the proposed framework outperforms the geometry algorithm even with only 2 anchors.

Fig. 7 illustrates the impact of the number of anchors and the size of the anchors on the performance of the proposed framework. To be specific, we present the comparison of the proposed framework with $N_y = N_z = 1$, $N_y = N_z = 2$, $N_y = N_z = 4$, and $N_y = N_z = 8$. As

it can be seen from Fig. 7, MSE decreases with the number of anchors. This implies that the positioning accuracy is better with a larger number of anchors. Furthermore, as shown in Fig. 7, there is a large gap between the curve of $N_y = N_z = 1$ and the curve of $N_y = N_z = 2$, while the curve of $N_y = N_z = 8$ is only a little better than the curve of $N_y = N_z = 4$. This implies that the impact of the anchor size becomes small when $N_y(N_z)$ is larger than 4.

IX. CONCLUSION

In this paper, we designed a comprehensive framework to analyze the angle estimation error and design the 3D positioning algorithm for the mmWave system. First, we estimated the AoAs at the anchors by applying the 2D-DFT algorithm. Based on the property of the 2D-DFT algorithm, the angle estimation error was analyzed in terms of PDF. We then simplified the intricate geometric expression of the error PDF by employing the first-order linear approximation of triangle functions. We also derived the variance expression of the error by using the error PDF and theoretically derived the variance from the error PDF. Finally, we applied the WLS algorithm to estimate the 3D position of the MU by using the estimated AoAs and the obtained non-Gaussian variance. Extensive simulation results confirmed that the derived angle estimation error is non-Gaussian, and also demonstrated the superiority of the proposed framework.

APPENDIX A
DERIVATION OF $D_{1,i}$

Firstly, we derive the expression of $D_{11,i}$ as

$$\begin{aligned}
D_{11,i} &= \frac{\hat{X}_i \alpha_{2,i}^2}{8a_i b_i \hat{Y}_i} \int_{B_{1,i}}^{B_{2,i}} (\hat{V}_i \tilde{\theta}_{L,i}^2 - \hat{U}_i \tilde{\theta}_{L,i}^3) d\tilde{\theta}_{L,i} - \frac{\hat{X}_i \beta_{1,i}^2}{8a_i b_i \hat{Y}_i} \int_{B_{1,i}}^{B_{2,i}} \frac{\hat{V}_i \tilde{\theta}_{L,i}^2 - \hat{U}_i \tilde{\theta}_{L,i}^3}{(\hat{U}_i + \hat{V}_i \tilde{\theta}_{L,i})^2} d\tilde{\theta}_{L,i} \\
&= \frac{\hat{X}_i \alpha_{2,i}^2}{8a_i b_i \hat{Y}_i} \int_{B_{1,i}}^{B_{2,i}} (\hat{V}_i \tilde{\theta}_{L,i}^2 - \hat{U}_i \tilde{\theta}_{L,i}^3) d\tilde{\theta}_{L,i} \\
&\quad - \left[\frac{\hat{X}_i \beta_{1,i}^2}{8a_i b_i \hat{Y}_i \hat{U}_i} \left(\int_0^{B_{2,i}} \frac{\hat{V}_i \tilde{\theta}_{L,i}^2}{(1 + \frac{\hat{V}_i \tilde{\theta}_{L,i}}{\hat{U}_i})^2} d\tilde{\theta}_{L,i} - \int_0^{B_{2,i}} \frac{\tilde{\theta}_{L,i}^3}{(1 + \frac{\hat{V}_i \tilde{\theta}_{L,i}}{\hat{U}_i})^2} d\tilde{\theta}_{L,i} \right) \right] \\
&= \frac{\hat{X}_i \alpha_{2,i}^2}{8a_i b_i \hat{Y}_i} \left(\frac{\hat{U}_i \tilde{\theta}_{L,i}^4}{4} - \frac{\hat{V}_i \tilde{\theta}_{L,i}^3}{3} \right) \Big|_{B_{1,i}}^{B_{2,i}} - \\
&\quad \left[\left(-\frac{\hat{X}_i \beta_{1,i}^2}{8a_i b_i \hat{Y}_i \hat{U}_i} \cdot \frac{B_{2,i}^4}{4} \cdot {}_2F_1 \left(2, 4; 5; -\frac{\hat{V}_i}{\hat{U}_i} B_{2,i} \right) + \frac{\hat{X}_i \beta_{1,i}^2 \hat{V}_i}{8a_i b_i \hat{Y}_i \hat{U}_i^2} \cdot \frac{B_{2,i}^3}{3} \cdot {}_2F_1 \left(2, 3; 4; -\frac{\hat{V}_i}{\hat{U}_i} B_{2,i} \right) \right) \right. \\
&\quad \left. - \left(-\frac{\hat{X}_i \beta_{1,i}^2}{8a_i b_i \hat{Y}_i \hat{U}_i} \cdot \frac{B_{1,i}^4}{4} \cdot {}_2F_1 \left(2, 4; 5; -\frac{\hat{V}_i}{\hat{U}_i} B_{1,i} \right) + \frac{\hat{X}_i \beta_{1,i}^2 \hat{V}_i}{8a_i b_i \hat{Y}_i \hat{U}_i^2} \cdot \frac{B_{1,i}^3}{3} \cdot {}_2F_1 \left(2, 3; 4; -\frac{\hat{V}_i}{\hat{U}_i} B_{1,i} \right) \right) \right], \tag{69}
\end{aligned}$$

where $\int_0^u \frac{x^{\mu-1} dx}{(1+\beta x)^v} = {}_2F_1 \left(\nu, \mu; 1 + \mu; -\beta u \right)$ is a generalized hypergeometric series [27].

Then, $D_{12,i}$ in (55) is derived as

$$D_{12,i} = \int_{B_{2,i}}^{B_{3,i}} \frac{\hat{X}_i (\hat{V}_i - \tilde{\theta}_{L,i} \hat{U}_i)}{2b} \tilde{\theta}_{L,i}^2 d\tilde{\theta}_{L,i} = \frac{\hat{X}_i}{2b_i} \left(\frac{\hat{V}_i \tilde{\theta}_{L,i}^3}{3} - \frac{\hat{U}_i \tilde{\theta}_{L,i}^4}{4} \right) \Big|_{B_{2,i}}^{B_{3,i}}. \tag{70}$$

Finally, $D_{13,i}$ in (55) is given by

$$\begin{aligned}
D_{13,i} &= \left[\left(-\frac{\hat{X}_i \beta_{2,i}^2}{8a_i b_i \hat{Y}_i \hat{U}_i} \cdot \frac{B_{4,i}^4}{4} \cdot {}_2F_1 \left(2, 4; 5; -\frac{\hat{V}_i}{\hat{U}_i} B_{4,i} \right) + \frac{\hat{X}_i \beta_{2,i}^2 \hat{V}_i}{8a_i b_i \hat{Y}_i \hat{U}_i^2} \cdot \frac{B_{4,i}^3}{3} \cdot {}_2F_1 \left(2, 3; 4; -\frac{\hat{V}_i}{\hat{U}_i} B_{4,i} \right) \right) \right. \\
&\quad \left. - \left(-\frac{\hat{X}_i \beta_{2,i}^2}{8a_i b_i \hat{Y}_i \hat{U}_i} \cdot \frac{B_{3,i}^4}{4} \cdot {}_2F_1 \left(2, 4; 5; -\frac{\hat{V}_i}{\hat{U}_i} B_{3,i} \right) + \frac{\hat{X}_i \beta_{2,i}^2 \hat{V}_i}{8a_i b_i \hat{Y}_i \hat{U}_i^2} \cdot \frac{B_{3,i}^3}{3} \cdot {}_2F_1 \left(2, 3; 4; -\frac{\hat{V}_i}{\hat{U}_i} B_{3,i} \right) \right) \right] \\
&\quad - \frac{\hat{X}_i \alpha_{1,i}^2}{8a_i b_i \hat{Y}_i} \left(-\frac{\hat{U}_i \tilde{\theta}_{L,i}^4}{4} + \frac{\hat{V}_i \tilde{\theta}_{L,i}^3}{3} \right) \Big|_{B_{3,i}}^{B_{4,i}}. \tag{71}
\end{aligned}$$

APPENDIX B
DERIVATION OF $D_{2,i}$

Firstly, $D_{21,i}$ in (56) is derived as

$$\begin{aligned}
D_{21,i} &= \frac{\hat{X}_i \alpha_{2,i}^2}{8a_i b_i \hat{Y}_i} \left(-\frac{\hat{U}_i \tilde{\theta}_{L,i}^3}{3} + \frac{\hat{V}_i \tilde{\theta}_{L,i}^2}{2} \right) \Big|_{B_{1,i}}^{B_{2,i}} \\
&\quad - \left[\left(-\frac{\hat{X}_i \beta_{1,i}^2}{8a_i b_i \hat{Y}_i \hat{U}_i} \cdot \frac{B_{2,i}^3}{3} \cdot {}_2F_1 \left(2, 3; 4; -\frac{\hat{V}_i}{\hat{U}_i} B_{2,i} \right) + \frac{\hat{X}_i \beta_{1,i}^2 \hat{V}_i}{8a_i b_i \hat{Y}_i \hat{U}_i^2} \cdot \frac{B_{2,i}^2}{2} \cdot {}_2F_1 \left(2, 2; 3; -\frac{\hat{V}_i}{\hat{U}_i} B_{2,i} \right) \right) \right. \\
&\quad \left. - \left(-\frac{\hat{X}_i \beta_{1,i}^2}{8a_i b_i \hat{Y}_i \hat{U}_i} \cdot \frac{B_{1,i}^3}{3} \cdot {}_2F_1 \left(2, 3; 4; -\frac{\hat{V}_i}{\hat{U}_i} B_{1,i} \right) + \frac{\hat{X}_i \beta_{1,i}^2 \hat{V}_i}{8a_i b_i \hat{Y}_i \hat{U}_i^2} \cdot \frac{B_{1,i}^2}{2} \cdot {}_2F_1 \left(2, 2; 3; -\frac{\hat{V}_i}{\hat{U}_i} B_{1,i} \right) \right) \right]. \tag{72}
\end{aligned}$$

Then, $D_{22,i}$ in (56) is written as

$$D_{22,i} = \int_{B_{2,i}}^{B_{3,i}} \frac{\hat{X}_i (\hat{V}_i - \tilde{\theta}_{L,i} \hat{U}_i)}{2b_i} \tilde{\theta}_{L,i} d\tilde{\theta}_{L,i} = \frac{\hat{X}_i}{2b_i} \left(-\frac{\hat{U}_i \tilde{\theta}_{L,i}^3}{3} + \frac{\hat{V}_i \tilde{\theta}_{L,i}^2}{2} \right) \Big|_{B_{2,i}}^{B_{3,i}}. \tag{73}$$

Finally, $D_{23,i}$ in (56) could be formulated as

$$\begin{aligned}
D_{23,i} &= \left[\left(-\frac{\hat{X}_i \beta_{2,i}^2}{8a_i b_i \hat{Y}_i \hat{U}_i} \cdot \frac{B_{4,i}^3}{3} \cdot {}_2F_1 \left(2, 3; 4; -\frac{\hat{V}_i}{\hat{U}_i} B_{4,i} \right) + \frac{\hat{X}_i \beta_{2,i}^2 \hat{V}_i}{8a_i b_i \hat{Y}_i \hat{U}_i^2} \cdot \frac{B_{4,i}^2}{2} \cdot {}_2F_1 \left(2, 2; 3; -\frac{\hat{V}_i}{\hat{U}_i} B_{4,i} \right) \right) \right. \\
&\quad \left. - \left(-\frac{\hat{X}_i \beta_{2,i}^2}{8a_i b_i \hat{Y}_i \hat{U}_i} \cdot \frac{B_{3,i}^3}{3} \cdot {}_2F_1 \left(2, 3; 4; -\frac{\hat{V}_i}{\hat{U}_i} B_{3,i} \right) + \frac{\hat{X}_i \beta_{2,i}^2 \hat{V}_i}{8a_i b_i \hat{Y}_i \hat{U}_i^2} \cdot \frac{B_{3,i}^2}{2} \cdot {}_2F_1 \left(2, 2; 3; -\frac{\hat{V}_i}{\hat{U}_i} B_{3,i} \right) \right) \right] \\
&\quad - \frac{\hat{X}_i \alpha_{1,i}^2}{8a_i b_i \hat{Y}_i} \left(-\frac{\hat{U}_i \tilde{\theta}_{L,i}^3}{3} + \frac{\hat{V}_i \tilde{\theta}_{L,i}^2}{2} \right) \Big|_{B_{3,i}}^{B_{4,i}}. \tag{74}
\end{aligned}$$

APPENDIX C
DERIVATION OF $D'_{1,i}$

As for $D'_{11,i}$ in (58), it could be expressed as

$$\begin{aligned}
D'_{11,i} &= \frac{\hat{X}_i \alpha_{2,i}^2}{8a_i b_i \hat{Y}_i} \left(-\frac{\hat{U}_i \tilde{\theta}_{L,i}^4}{4} + \frac{\hat{V}_i \tilde{\theta}_{L,i}^3}{3} \right) \Big|_{B_{1,i}}^{B_{3,i}} - \\
&\quad \left[\left(-\frac{\hat{X}_i \beta_{1,i}^2}{8a_i b_i \hat{Y}_i \hat{U}_i} \cdot \frac{B_{3,i}^4}{4} \cdot {}_2F_1 \left(2, 4; 5; -\frac{\hat{V}_i}{\hat{U}_i} B_{3,i} \right) + \frac{\hat{X}_i \beta_{1,i}^2 \hat{V}_i}{8a_i b_i \hat{Y}_i \hat{U}_i^2} \cdot \frac{B_{3,i}^3}{3} \cdot {}_2F_1 \left(2, 3; 4; -\frac{\hat{V}_i}{\hat{U}_i} B_{3,i} \right) \right) \right. \\
&\quad \left. - \left(-\frac{\hat{X}_i \beta_{1,i}^2}{8a_i b_i \hat{Y}_i \hat{U}_i} \cdot \frac{B_{1,i}^4}{4} \cdot {}_2F_1 \left(2, 4; 5; -\frac{\hat{V}_i}{\hat{U}_i} B_{1,i} \right) + \frac{\hat{X}_i \beta_{1,i}^2 \hat{V}_i}{8a_i b_i \hat{Y}_i \hat{U}_i^2} \cdot \frac{B_{1,i}^3}{3} \cdot {}_2F_1 \left(2, 3; 4; -\frac{\hat{V}_i}{\hat{U}_i} B_{1,i} \right) \right) \right]. \tag{75}
\end{aligned}$$

Then, $D'_{12,i}$ in (58) is given by

$$D'_{12,i} = \left(-\frac{\hat{X}_i \hat{Z}_i}{2a \hat{Y}_i \hat{U}_i} \cdot \frac{B_{2,i}^4}{4} \cdot {}_2F_1\left(2, 4; 5; -\frac{\hat{V}_i}{\hat{U}_i} B_{2,i}\right) + \frac{\hat{X}_i \hat{Z}_i \hat{V}_i}{2a \hat{Y}_i \hat{U}_i^2} \cdot \frac{B_{2,i}^3}{3} \cdot {}_2F_1\left(2, 3; 4; -\frac{\hat{V}_i}{\hat{U}_i} B_{2,i}\right) \right) \\ - \left(-\frac{\hat{X}_i \hat{Z}_i}{2a \hat{Y}_i \hat{U}_i} \cdot \frac{B_{3,i}^4}{4} \cdot {}_2F_1\left(2, 4; 5; -\frac{\hat{V}_i}{\hat{U}_i} B_{3,i}\right) + \frac{\hat{X}_i \hat{Z}_i \hat{V}_i}{2a \hat{Y}_i \hat{U}_i^2} \cdot \frac{B_{3,i}^3}{3} \cdot {}_2F_1\left(2, 3; 4; -\frac{\hat{V}_i}{\hat{U}_i} B_{3,i}\right) \right). \quad (76)$$

Finally, $D'_{13,i}$ in (58) is derived as

$$D'_{13,i} = \left[\left(-\frac{\hat{X}_i \beta_{2,i}^2}{8a_i b_i \hat{Y}_i \hat{U}_i} \cdot \frac{B_{4,i}^4}{4} \cdot {}_2F_1\left(2, 4; 5; -\frac{\hat{V}_i}{\hat{U}_i} B_{4,i}\right) + \frac{\hat{X}_i \beta_{2,i}^2 \hat{V}_i}{8a_i b_i \hat{Y}_i \hat{U}_i^2} \cdot \frac{B_{4,i}^3}{3} \cdot {}_2F_1\left(2, 3; 4; -\frac{\hat{V}_i}{\hat{U}_i} B_{4,i}\right) \right) \right. \\ \left. - \left(-\frac{\hat{X}_i \beta_{2,i}^2}{8a_i b_i \hat{Y}_i \hat{U}_i} \cdot \frac{B_{2,i}^4}{4} \cdot {}_2F_1\left(2, 4; 5; -\frac{\hat{V}_i}{\hat{U}_i} B_{2,i}\right) + \frac{\hat{X}_i \beta_{2,i}^2 \hat{V}_i}{8a_i b_i \hat{Y}_i \hat{U}_i^2} \cdot \frac{B_{2,i}^3}{3} \cdot {}_2F_1\left(2, 3; 4; -\frac{\hat{V}_i}{\hat{U}_i} B_{2,i}\right) \right) \right] \\ - \frac{\hat{X}_i \alpha_{1,i}^2}{8a_i b_i \hat{Y}_i} \left(-\frac{\hat{U}_i \tilde{\theta}_{L,i}^4}{4} + \frac{\hat{V}_i \tilde{\theta}_{L,i}^3}{3} \right) \Big|_{B_{2,i}}^{B_{4,i}}. \quad (77)$$

APPENDIX D

DERIVATION OF $D'_{2,i}$

Firstly, $D'_{21,i}$ in (59) is formulated as

$$D'_{21,i} = \frac{\hat{X}_i \alpha_{2,i}^2}{8a_i b_i \hat{Y}_i} \left(-\frac{\hat{U}_i \tilde{\theta}_{L,i}^3}{3} + \frac{\hat{V}_i \tilde{\theta}_{L,i}^2}{2} \right) \Big|_{B_{1,i}}^{B_{3,i}} - \\ \left[\left(-\frac{\hat{X}_i \beta_{1,i}^2}{8a_i b_i \hat{Y}_i \hat{U}_i} \cdot \frac{B_{3,i}^3}{3} \cdot {}_2F_1\left(2, 3; 4; -\frac{\hat{V}_i}{\hat{U}_i} B_{3,i}\right) + \frac{\hat{X}_i \beta_{1,i}^2 \hat{V}_i}{8a_i b_i \hat{Y}_i \hat{U}_i^2} \cdot \frac{B_{3,i}^2}{2} \cdot {}_2F_1\left(2, 2; 3; -\frac{\hat{V}_i}{\hat{U}_i} B_{3,i}\right) \right) \right. \\ \left. - \left(-\frac{\hat{X}_i \beta_{1,i}^2}{8a_i b_i \hat{Y}_i \hat{U}_i} \cdot \frac{B_{1,i}^3}{3} \cdot {}_2F_1\left(2, 3; 4; -\frac{\hat{V}_i}{\hat{U}_i} B_{1,i}\right) + \frac{\hat{X}_i \beta_{1,i}^2 \hat{V}_i}{8a_i b_i \hat{Y}_i \hat{U}_i^2} \cdot \frac{B_{1,i}^2}{2} \cdot {}_2F_1\left(2, 2; 3; -\frac{\hat{V}_i}{\hat{U}_i} B_{1,i}\right) \right) \right]. \quad (78)$$

Then, $D'_{22,i}$ in (59) is written as

$$D'_{22,i} = \left(-\frac{\hat{X}_i \hat{Z}_i}{2a \hat{Y}_i \hat{U}_i} \cdot \frac{B_{2,i}^3}{3} \cdot {}_2F_1\left(2, 3; 4; -\frac{\hat{V}_i}{\hat{U}_i} B_{2,i}\right) + \frac{\hat{X}_i \hat{Z}_i \hat{V}_i}{2a \hat{Y}_i \hat{U}_i^2} \cdot \frac{B_{2,i}^2}{2} \cdot {}_2F_1\left(2, 2; 3; -\frac{\hat{V}_i}{\hat{U}_i} B_{2,i}\right) \right) \\ - \left(-\frac{\hat{X}_i \hat{Z}_i}{2a \hat{Y}_i \hat{U}_i} \cdot \frac{B_{3,i}^3}{3} \cdot {}_2F_1\left(2, 3; 4; -\frac{\hat{V}_i}{\hat{U}_i} B_{3,i}\right) + \frac{\hat{X}_i \hat{Z}_i \hat{V}_i}{2a \hat{Y}_i \hat{U}_i^2} \cdot \frac{B_{3,i}^2}{2} \cdot {}_2F_1\left(2, 2; 3; -\frac{\hat{V}_i}{\hat{U}_i} B_{3,i}\right) \right). \quad (79)$$

Finally, $D'_{23,i}$ in (59) is obtained as

$$\begin{aligned}
D'_{23,i} = & \left[\left(-\frac{\hat{X}_i \beta_{2,i}^2}{8a_i b_i \hat{Y}_i \hat{U}_i} \cdot \frac{B_{4,i}^3}{3} \cdot {}_2F_1\left(2, 3; 4; -\frac{\hat{V}_i}{\hat{U}_i} B_{4,i}\right) + \frac{\hat{X}_i \beta_{2,i}^2 \hat{V}_i}{8a_i b_i \hat{Y}_i \hat{U}_i^2} \cdot \frac{B_{4,i}^2}{2} \cdot {}_2F_1\left(2, 2; 3; -\frac{\hat{V}_i}{\hat{U}_i} B_{4,i}\right) \right) \right. \\
& - \left. \left(-\frac{\hat{X}_i \beta_{2,i}^2}{8a_i b_i \hat{Y}_i \hat{U}_i} \cdot \frac{B_{2,i}^3}{3} \cdot {}_2F_1\left(2, 3; 4; -\frac{\hat{V}_i}{\hat{U}_i} B_{2,i}\right) + \frac{\hat{X}_i \beta_{2,i}^2 \hat{V}_i}{8a_i b_i \hat{Y}_i \hat{U}_i^2} \cdot \frac{B_{2,i}^2}{2} \cdot {}_2F_1\left(2, 2; 3; -\frac{\hat{V}_i}{\hat{U}_i} B_{2,i}\right) \right) \right] \\
& - \frac{\hat{X}_i \alpha_{1,i}^2}{8a_i b_i \hat{Y}_i} \left(-\frac{\hat{U}_i \tilde{\theta}_{L,i}^3}{3} + \frac{\hat{V}_i \tilde{\theta}_{L,i}^2}{2} \right) \Big|_{B_{2,i}}^{B_{4,i}}. \tag{80}
\end{aligned}$$

REFERENCES

- [1] Y. Zhou, L. Liu, L. Wang, N. Hui, X. Cui, J. Wu, Y. Peng, Y. Qi, and C. Xing, "Service-aware 6G: An intelligent and open network based on the convergence of communication, computing and caching," *Digit. Commun. Netw.*, 2020.
- [2] Z. Zhang, Y. Xiao, Z. Ma, M. Xiao, Z. Ding, X. Lei, G. K. Karagiannidis, and P. Fan, "6G Wireless Networks: Vision, Requirements, Architecture, and Key Technologies," *IEEE Commun. Mag.*, vol. 14, no. 3, pp. 28–41, 2019.
- [3] H. Ren, K. Wang, and C. Pan, "Intelligent Reflecting Surface-Aided URLLC in a Factory Automation Scenario," *IEEE Trans. Commun.*, vol. 70, no. 1, pp. 707–723, 2022.
- [4] F. Hu, Y. Deng, W. Saad, M. Bennis, and A. H. Aghvami, "Cellular-Connected Wireless Virtual Reality: Requirements, Challenges, and Solutions," *IEEE Commun. Mag.*, vol. 58, no. 5, pp. 105–111, 2020.
- [5] T. G. Reid, S. E. Houts, R. Cammarata, G. Mills, S. Agarwal, A. Vora, and G. Pandey, "Localization Requirements for Autonomous Vehicles," *SAE International Jour. of Conn. and Auto. Veh.*, vol. 2, no. 3, sep 2019.
- [6] H. Srieddeen, N. Saeed, T. Y. Al-Naffouri, and M.-S. Alouini, "Next Generation Terahertz Communications: A Rendezvous of Sensing, Imaging, and Localization," *IEEE Commun. Mag.*, vol. 58, no. 5, pp. 69–75, 2020.
- [7] R. Mendrzik, F. Meyer, G. Bauch, and M. Z. Win, "Enabling Situational Awareness in Millimeter Wave Massive MIMO Systems," *IEEE J. Sel. Topics Signal Process.*, vol. 13, no. 5, pp. 1196–1211, 2019.
- [8] H. Liu, H. Darabi, P. Banerjee, and J. Liu, "Survey of Wireless Indoor Positioning Techniques and Systems," *IEEE Trans. on Sys., Man, and Cyber., Part C (Applications and Reviews)*, vol. 37, no. 6, pp. 1067–1080, 2007.
- [9] C. Pan, H. Ren, K. Wang, J. F. Kolb, M. El-kashlan, M. Chen, M. Di Renzo, Y. Hao, J. Wang, A. L. Swindlehurst, X. You, and L. Hanzo, "Reconfigurable Intelligent Surfaces for 6G Systems: Principles, Applications, and Research Directions," *IEEE Commun. Mag.*, vol. 59, no. 6, pp. 14–20, 2021.
- [10] D. Dardari, P. Closas, and P. M. Djurić, "Indoor Tracking: Theory, Methods, and Technologies," *IEEE Trans. Veh. Technol.*, vol. 64, no. 4, pp. 1263–1278, 2015.
- [11] Q. Li, B. Chen, and M. Yang, "Improved Two-Step Constrained Total Least-Squares TDOA Localization Algorithm Based on the Alternating Direction Method of Multipliers," *IEEE Sensors Journal*, vol. 20, no. 22, pp. 13 666–13 673, 2020.
- [12] D. Fan, F. Gao, Y. Liu, Y. Deng, G. Wang, Z. Zhong, and A. Nallanathan, "Angle Domain Channel Estimation in Hybrid Millimeter Wave Massive MIMO Systems," *IEEE Trans. Wireless Commun.*, vol. 17, no. 12, pp. 8165–8179, 2018.
- [13] S. Rao, A. Mezghani, and A. L. Swindlehurst, "Channel Estimation in One-Bit Massive MIMO Systems: Angular Versus Unstructured Models," *IEEE J. Sel. Topics Signal Process.*, vol. 13, no. 5, pp. 1017–1031, 2019.

- [14] R. Ramlall, J. Chen, and A. L. Swindlehurst, “Non-line-of-sight mobile station positioning algorithm using TOA, AOA, and Doppler-shift,” in *2014 Ubiquitous Positioning Indoor Navigation and Location Based Service (UPINLBS)*, 2014, pp. 180–184.
- [15] C. Hu, L. Dai, S. Han, and X. Wang, “Two-Timescale Channel Estimation for Reconfigurable Intelligent Surface Aided Wireless Communications,” *IEEE Trans. Commun.*, vol. 69, no. 11, pp. 7736–7747, 2021.
- [16] Z. Lin, T. Lv, and P. T. Mathiopoulos, “3-D Indoor Positioning for Millimeter-Wave Massive MIMO Systems,” *IEEE Trans. Commun.*, vol. 66, no. 6, pp. 2472–2486, 2018.
- [17] B. Zhou, A. Liu, and V. Lau, “Successive Localization and Beamforming in 5G mmWave MIMO Communication Systems,” *IEEE Trans. Signal Process.*, vol. 67, no. 6, pp. 1620–1635, 2019.
- [18] J. He, H. Wymeersch, L. Kong, O. Silvén, and M. Juntti, “Large intelligent surface for positioning in millimeter wave MIMO systems,” in *2020 IEEE 91st Veh. Technol. Conf.*, 2020, pp. 1–5.
- [19] A. Elzanaty, A. Guerra, F. Guidi, and M.-S. Alouini, “Reconfigurable Intelligent Surfaces for Localization: Position and Orientation Error Bounds,” *IEEE Trans. Signal Process.*, vol. 69, pp. 5386–5402, 2021.
- [20] O. Kanhere and T. S. Rappaport, “Position Locationing for Millimeter Wave Systems,” in *2018 IEEE Glob. Commun. Conf. (GLOBECOM)*, 2018, pp. 206–212.
- [21] Y. Lin, S. Jin, M. Matthaiou, and X. You, “Channel Estimation and User Localization for IRS-Assisted MIMO-OFDM Systems,” *IEEE Trans. Wireless Commun.*, vol. 21, no. 4, pp. 2320–2335, 2022.
- [22] G. Zhou, C. Pan, H. Ren, P. Popovski, and A. L. Swindlehurst, “Channel estimation for RIS-aided multiuser millimeter-wave systems,” *IEEE Trans. Signal Process.*, vol. 70, pp. 1478–1492, 2022.
- [23] E. Basar, M. Di Renzo, J. De Rosny, M. Debbah, M.-S. Alouini, and R. Zhang, “Wireless communications through reconfigurable intelligent surfaces,” *IEEE Access*, vol. 7, pp. 116 753–116 773, 2019.
- [24] X. Y. Yang and B. X. Chen, “A High-Resolution Method for 2D DOA Estimation,” *J. Elect. and Inf. Tech.*, vol. 32, no. 4, pp. 953–958, 2010.
- [25] T. Wu, C. Pan, Y. Pan, S. Hong, H. Ren, M. ElKashlan, F. Shu, and J. Wang, “3D Positioning Algorithm Design for RIS-aided mmWave Systems,” 2022. [Online]. Available: <https://arxiv.org/abs/2208.07606>
- [26] H. Wymeersch and B. Denis, “Beyond 5G Wireless Localization with Reconfigurable Intelligent Surfaces,” in *ICC 2020 - 2020 IEEE International Conf. Commun. (ICC)*, 2020, pp. 1–6.
- [27] I. S. Gradshteyn and I. M. Ryzhik, “Table of integrals, series, and products,” *Mathematics of Computation*, vol. 20, no. 96, p. 1157, 2007.